LUND UNIVERSITY

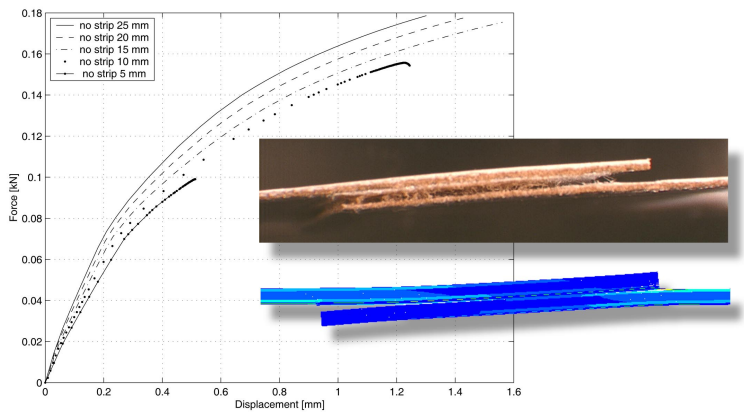

LONGITUDINAL SEALINGS IN BEVERAGE PACKAGES - Experimental Testing and Numerical Parameter Studies

MAGNUS NILSSON

Structural Mechanics

Master's Dissertation

Structural Mechanics

ISRN LUTVDG/TVSM--05/5134--SE (1-95)
ISSN 0281-6679

LONGITUDINAL SEALINGS IN BEVERAGE PACKAGES - Experimental Testing and Numerical Parameter Studies

Master's Dissertation by

Magnus Nilsson

Supervisors:

Kent Persson, Div. of Structural Mechanics

Eskil Andreasson, Tetra Pak R&D AB, Lund

Printed by KFS I Lund AB, Lund, Sweden, December, 2005.

For information, address:
Division of Structural Mechanics, LTH, Lund University, Box 118, SE-221 00 Lund, Sweden.
Homepage: http://www.byggmek.lth.se

Abstract

In this work, the mechanical behavior of longitudinal sealings in paper based beverage packages have been investigated trough experimental tests and Finite Element simulations. The mechanical performance of the longitudinal sealing is of great interest when developing and improving beverage packages. Choosing a suitable sealing type is both a performance and cost issue, therefore is better knowledge of the mechanical behavior of great interest.

Experimental tension tests were accomplished on various longitudinal sealings in order to determine the response of the sealing. FE-simulations of the sealings with the 3DM employed were modelled in ABAQUS and further on were numerical parametric studies with focus on geometry and material properties performed. The simulations gave quite accurate predictions of the initial mechanical behavior and the plastic hardening when the 3DM was employed, but the ultimate strength was in some cases difficult to capture.

The weak region when a package sealing is subjected to loading is the paperboard and not the actual sealing. Stresses in the thickness direction and shear stresses initiate a crack in the paperboard, which then propagates in the length dimension and eventually causes failure in the paperboard. A new type of sealing, the edge to edge sealing, was studied with FE-simulations in ABAQUS. This sealing differs from the existing sealings by not being an overlap sealing. Stresses do not occur in the same extension in the thickness direction in an edge to edge sealing as in an overlap sealing, due to the lack of rotation of the symmetric cross section. Therefore it is possible for the edge to edge sealing to be subjected to higher loads.

Acknowledgements

The research presented in this master´s thesis was carried out at the Division of Structural Mechanics, LTH, Lund University, Sweden in cooperation with Tetra Pak R&D AB in Lund during March to October 2005.

I give my sincere appreciation and gratitude to my supervisors Ph.D. Kent Persson at the Division of Structural Mechanics and M.Sc. Eskil Andreasson at Tetra Pak R&D AB for their guidance, invaluable advice and support during this work.

I am also very grateful to Håkan Andersson, Tommy Jönsson and Daniella Nae at Tetra Pak R&D AB for their help with the experimental tests and to Mr Bo Zadig at the Division of Structural Mechanics for his help with the cover of this report.

Lund, November 2005

Magnus Nilsson

Contents

Chapter 1

Introduction

1.1 Background

The use of paper based beverage packages throughout the world is nowadays widely spread. Tetra Pak launched their first functional paper based beverage package, the tetrahedon-shaped carton, in 1952 [10]. Since the mid 90's Tetra Pak has been one of the leading companies within this field. In order to continue being one of the leading companies, it is necessary to widen the supply of beverage packages within new areas of packaging types and to improve existing packages. To be able to do this one of the areas to be studied is for instance the mechanical behavior of the longitudinal sealing (abbreviation LS). The LS extends in the vertical direction of the package, which is shown in Figure 1.1. To improve the strength and to be able to choose the correct strength of the LS for various packages, a wider knowledge of the mechanical behavior of the LS is of great interest.

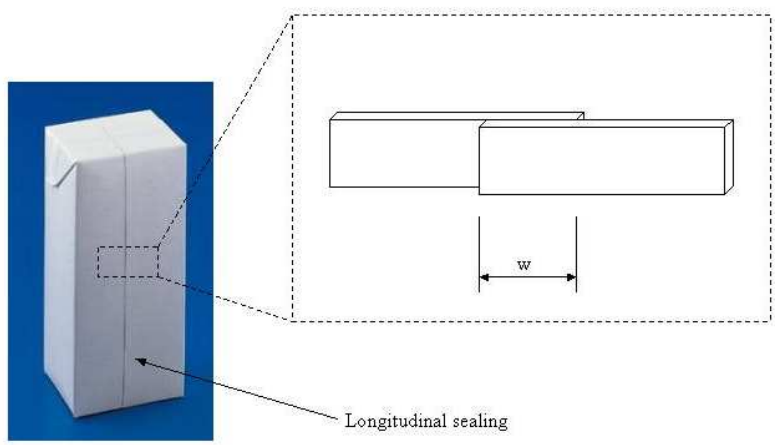

Figure 1.1: *Longitudinal sealing and longitudinal overlap width, w*

1.2 Problem formulation

This work primarily focus on the difference in mechanical behavior between various LS types and how the longitudinal overlap width (shown in Figure 1.1) affects the strength of the LS. When paper is subjected to loading in the thickness dimension, it starts to delaminate as shown in Figure 1.2. To be able to implement delamination as well as in-plane material plasticity in the models, a material model for paper, the 3DM [5], will be adopted. The 3DM adopted in this report is investigated for other load cases than the folding and creasing operations it is originally written and tested for. The model was written in order to predict and govern delamination. Delamination makes it easier to fold the package to its final shape and is therefore desirable in some regions. However, in the LS, delamination causes crack initiation which eventually is the reason for fracture and by that leakage in the package.

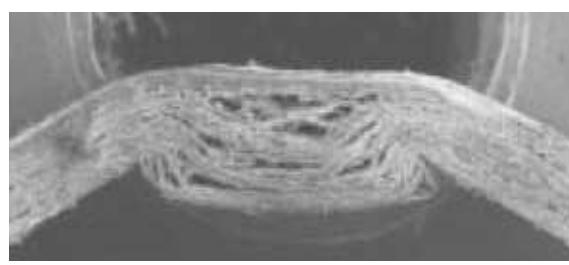

Figure 1.2: *The phenomenon of delamination*

1.3 Objectives

The main objectives of this work was to increase the knowledge of which factors that influence the mechanical behavior of the LS the most. This was accomplished through experimental tests of longitudinal sealings and furthermore was the behavior of various LS setups predicted with FE-models implemented in ABAQUS. A numerical parametric study was accomplished to investigate which possible parameters that influence the mechanical behavior of the sealings the most.

1.4 Scope of the thesis

In chapter 2 are packages and various longitudinal sealings presented. Chapter 3 consists of the experimental tests performed. In chapter 4 is the FEM and the material models employed explained and in chapter 5 are the finite element simulations presented. In chapter 6 are the various numerical studies presented and finally in chapter 7 are the results from this work discussed.

Chapter 2

Beverage packages and longitudinal sealings

2.1 General remarks

Since the first packaging machine was sold in 1952 Tetra Pak has developed a great many different package types, mostly for liquid beverages, but also for food [10]. In Figure 2.1 are the most common packages shown. The various packages are supposed to appeal different segment of customers. There are i.e rather cheap packages as Tetra Fino Aseptic without any bottom and top folding and more exclusive ones as Tetra Prisma Aseptic.

Figure 2.1: *Tetra Pak packages, from the left to the right: Tetra Classic, Tetra Wedge, Tetra Rex, Tetra Prisma, Tetra Brik, Tetra Fino, Tetra Top, PET bottles and EBM bottles [3]*

2.2 Materials in a package

The package material used in this work is a laminate structure consisting of (outside-inside) Low Density Polyethylene (LDPE), 260 mN paperboard, LDPE, aluminum foil and polymer film c.f Figure 2.2. The aluminum foil layer is located at the inside to create aseptic packages that are sustainable, non diffusive and that protects the beverage from light. LDPE layers are applied to protect the paper from moisture, to protect the printing and to glue the aluminum foil and the paper together. Since it is the paperboard that is crucial for the strength of the LS, it is more thoroughly considered than the other materials in this report. Tetra Pak have chosen to measure the quality of the paperboard with bending stiffness, which in this case is 260 $mN\frac{m}{m}$. The bending stiffness is measured per meter and therefore is the unit $[N]$.

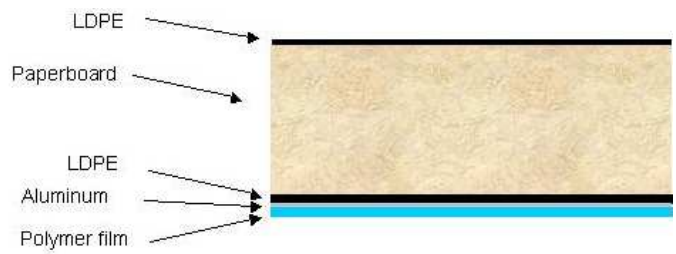

Figure 2.2: *The laminate*

Most paperboard materials used in a package are layered with one mechanical pulp and two chemical pulps. The mechanical pulp is placed as a middle layer with chemical pulps on the sides. The chemical pulp is of higher strength and is therefore placed in the outer layers in order to stiffen the paperboard for bending. Paper is due to the manufacturing process orthotropic with substantial varying material properties in the different material directions. The three material directions are the Machine Direction (MD), Cross Direction (CD) and out-of-plane direction (ZD), see Figure 2.3. The strength in the thickness direction, ZD, is about hundred times lower compared to the strength in MD, which causes problem in the LS. The behavior of the LS highly depends on how the paper is oriented. Most beverage packages from Tetra Pak have due to machine reasons MD oriented in the vertical height direction and therefore CD oriented in the horizontal width dimension, see Figure 2.3. This makes the LS less strong but also less ductile of fracture.

Since the strength in ZD is very modest, it will break in this direction even for very small stresses. Stresses develop in the ZD when the LS is loaded in the CD, due to the overlap sealing which rotates the cross section as shown in Figure 2.4. A LS type which could decrease the stresses in the ZD would probably manage to increase the strength significantly.

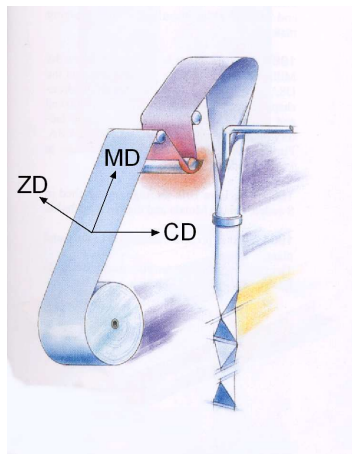

Figure 2.3: *The different directions in paper material.*

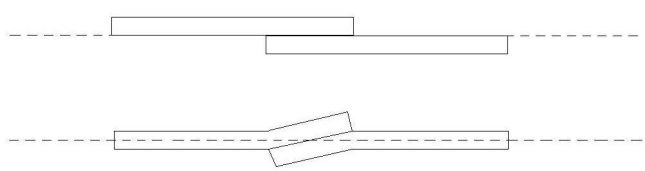

Figure 2.4: *Change of cross section when the LS is loaded in the horizontal length direction*

2.3 Induction heating

The sealing process in longitudinal sealings is often based on induction heating. The induction heating system mainly consists of two parts, the inductor and the work piece. The inductor is a copper coil, which lies in a plastic inductor compound as presented in Figure 2.5. The work piece is in this case the aluminium foil in the

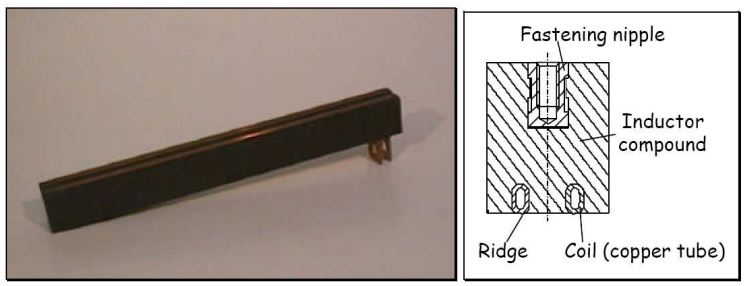

Figure 2.5: *Inductor [2]*

package material. The inductor is placed, under pressure, on the outside of the package material. When high frequency current is running through the copper coil an alternating magnetic field is created. This magnetic field induces an opposing current in the aluminium foil which, due to the resistance in the aluminium, causes heating. The principle of induction heating is presented in Figure 2.6.

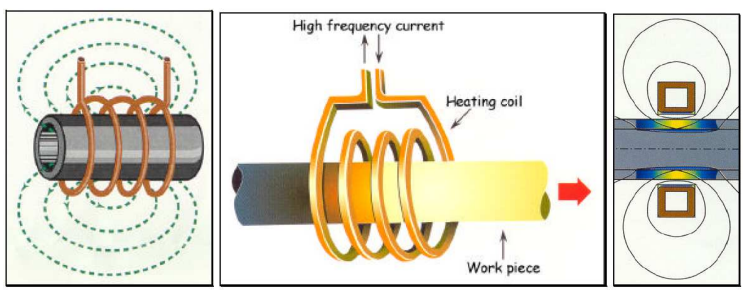

Figure 2.6: *The principle of induction heating [2].*

The heat melts the LDPE material and the polymer film which glues the package material together. This heating method is used because it is possible to rather precisely control the location of the heat in the material and because of its high efficiency.

2.4 Various longitudinal sealings

Four types of various sealing setups were modelled and simulated in ABAQUS [1]. Two of them are used at Tetra Pak whereas the others are used only in this work. The various sealing setups are shown in Figure 2.7.

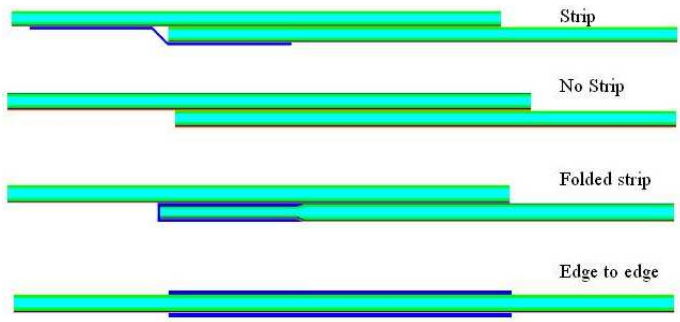

Figure 2.7: *Various sealing setups from the top to the bottom: strip, no strip, folded strip and edge to edge*

2.4.1 Strip

The most frequently sealing setup used in packages that currently are produced by Tetra Pak, is the *strip* sealing. A strip is glued over the sealing on the inside of the package to protect the paperboard from moisture that negatively affects the mechanical properties of paper.

2.4.2 No Strip

When creating models in ABAQUS it is convenient to develop models that easily can be modified. When making experimental work it is of great advantage to test parameter variations on the simplest possible specimen to exclude as many disturbing factors as possible. Due to these reasons, the sealing setup *no strip* was in most cases chosen for extensive studies. In real packages it is inconvenient to exclude the strip and have a carton edge not secured from the beverage in the package, thus is the appearance of the *no strip* sealing due to its simplicity in modelling.

2.4.3 Folded Strip

Folded strip is currently used in some commercial beverage packages at Tetra Pak. When manufacturing packages it is easier to have a strip that is folded around the edge of the laminate, instead of an ordinary strip described in section 2.4.1. When certain packages are produced in the machine, the strip often begins to flap, which

may cause machine stop. If the strip is folded around the edge of the laminate, this problem is eliminated.

2.4.4 Edge To Edge

Edge to edge is a completely new sealing type never produced. Because of the ordinary overlap sealing used in all beverage packages, stresses develop in the thickness direction ZD, which causes problems regarding the strength of the sealing. This new sealing type, which is not an overlap sealing and therefore does not cause a rotation of the cross section, can perhaps solve this problem and increase the strength of the sealing. On the other hand is this sealing type probably quite difficult to manufacture because of the edges on the laminate which must be tight to each other as shown in Figure 2.7.

Chapter 3

Experimental work

3.1 General remarks

In order to determine the mechanical behavior of the longitudinal sealing in packages, six various experimental tension tests were carried out in the paper laboratory at Tetra Pak R&D AB in Lund. The tension tests were performed on specimens sealed together with various overlap widths and sealing types. The various tests performed are shown in Table 3.1.

3.2 Specimens

The paperboard used in all experimental tests was a 260 mN three ply board. Sheets of the laminate packaging material were cut to desired dimensions in order to receive correct overlap widths of the LS. The sheets were then put in a package rig which created the sealing. When the LS was made the specimens were cut to a length of 150 mm and a width of 15 mm and were then conditioned at a predefined climate with a temperature of 23°C and a relative humidity of 50 %, for at least 72 hours. A typical specimen is shown in Figure 3.1. It was rather difficult to receive the overlap widths desired in the package rig. The difference between the desired widths and the actual measured widths were in some cases substantial. In Section 3.3 are the desired widths presented and in Section 3.5 are the measured widths presented in the diagrams.

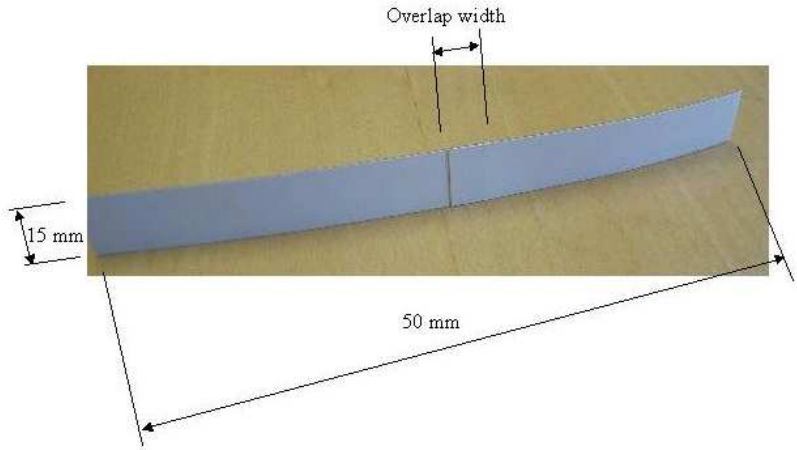

Figure 3.1: *A typical specimen*

3.3 Test series

In the first test series was the sample size chosen to ten, but since the variance was small, which is shown in the figures in Appendix A, the sample size was decreased to six in the following test series. In the first test series, five different overlap widths

Table 3.1: Experimental tests

Test series	*Characteristic*	*Number of samples*
1	No strip, overlap widths 6-24 mm	10 per overlap width
2	No strip, overlap widths 8-11 mm	6 per overlap width
3	Strip and Folded strip	6 per sealing type
4	Material direction CD,MD	6 per material direction
5	Setup with an unsatisfactory sealing	6
6	Laminate test	6

with rather large span between the widths were tested. This was carried out to investigate the influence of the overlap width on the strength of the sealing. The overlap widths tested were 6, 9, 12, 18 and 24 mm, and the sealing type was *no strip*, c.f Figure 2.7.

In the second test series the sealing type *no strip* was tested again, but now with overlap widths of 8, 9, 10 and 11 mm. This was made since it was found that there was a substantial increase in the ultimate strength at these overlap widths.

In the third test series, specimens with the sealing types *strip* and *folded strip* (c.f Figure 2.7) were tested, see Table 3.2 for the various cases. The specimens made in the package rig are denoted case one and the specimens made in an actual package machine are denoted case two. The specimens cut up from juice packages bought in an ordinary store are denoted case three and case four. The test of the juice packages were accomplished in order to investigate if there were any aging effects influencing the mechanical behavior of the sealing to consider.

Table 3.2: Tests made in the third test series

Notation	*Overlap width* [mm]	*Characteristic*	*Thickness of laminate* [μm]
Case one: machine package	9	folded strip	0.467
Case two: rig package	9	folded strip	0.467
Case three: juice package	8	strip	0.458
Case four: juice package	7	strip	0.492

In the fourth test series the influence of the material direction on the strength of the sealing was tested. Specimens with 10 mm overlap width were tested with both MD and CD oriented in the horizontal length dimension.

In the fifth test series specimens with an overlap width of 18 mm and a channel of 6 mm in the middle, which was not sealed, was tested, c.f Figure 3.2. This was carried out in order to investigate if an unsatisfactory performed sealing in the middle affects the overall mechanical behavior of the sealing.

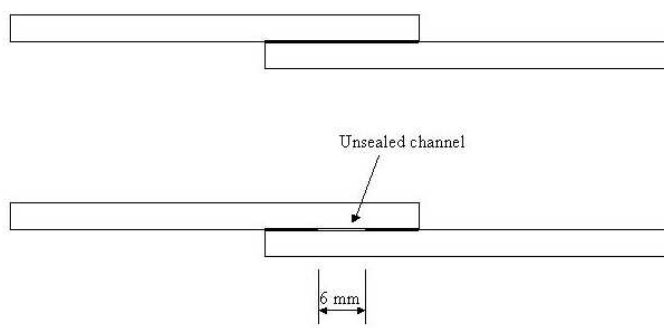

Figure 3.2: *The upper picture shows a satisfactory sealing and the lower picture shows an unsatisfactory sealing with an unsealed channel of six mm*

In the sixth test series the laminate used in this work was tested in order to investigate if the mechanical behavior of the various sealings was the differing from the behavior of the laminate.

3.4 Experimental setup

To determine the force versus the displacement of the specimens in test series one to six, a tension test was performed. The tests were carried out using an Instron tensile testing machine with hydraulic clamps shown in Figure 3.3. The lower clamp was fully constrained whereas the upper clamp was free to move horizontally. All specimens were placed in the machine with a free length of 50 mm and the sealing in the middle. The upper clamp moved with a crosshead speed of $10mm/minute$ until failure occurred in the specimen. The force and the displacement were recorded and plotted by a computer connected to the Instron machine.

3.5 Results

All curves presented in the graphs below are mean value curves of the experimental tests. A more thorough presentation of the curves can be found in Appendix A.The actually sealed widths were measured on one specimen for each width. Unfortunately there was a great deal of difference between the desired width and the measured

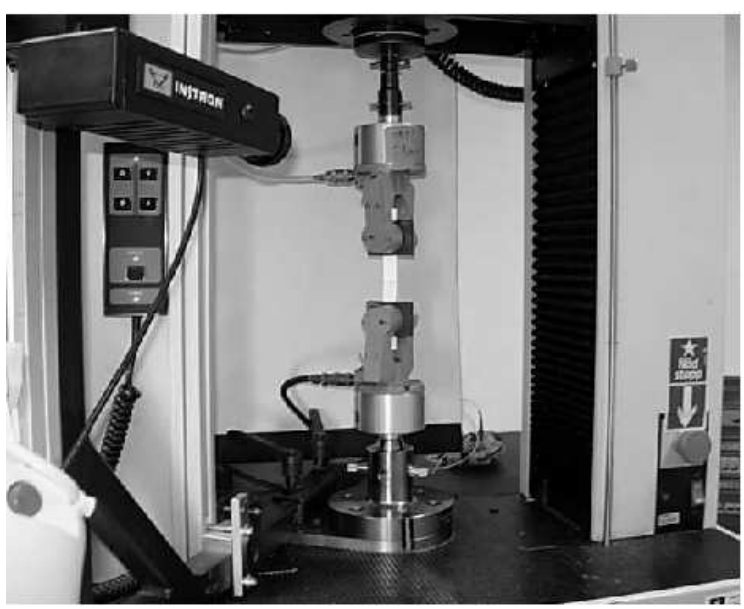

Figure 3.3: *Test setup for the tensile testing.*

width in numerous cases, therefore are the measured widths presented in the graphs.

3.5.1 Test series 1 - overlap widths

Figure 3.4 shows the force - displacement mean value curves of the overlap widths examined in test series 1. All curves for all overlap widths show similar behavior until the ultimate strength is reached. The specimens with the overlap width 6.2 mm shows a behavior beyond the ultimate strength that is somewhat different with a plateau region in the fracturing part of the force - displacement curve. This is probably due to that the small size of the overlap width enables a more stable fracture to occur.

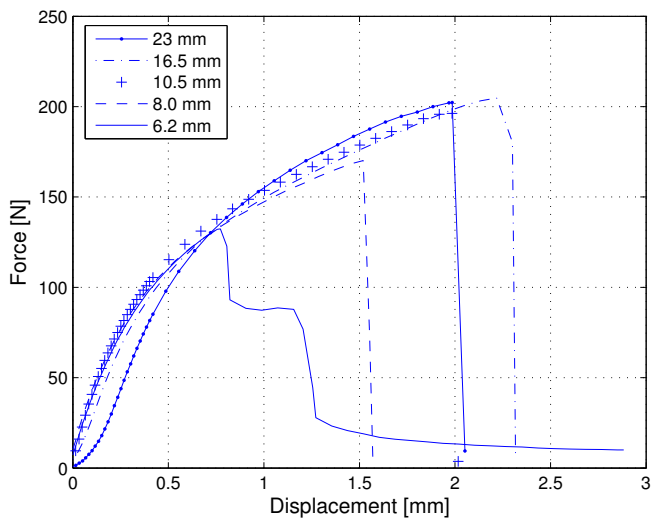

Figure 3.4: *Mean value curves from test series 1.*

3.5.2 Test series 2 - overlap widths

Since there was a substantial increase in strength between the overlap widths of 6.2 and 10.5 mm, test series 2 was carried out with smaller increments between the overlap widths. Figure 3.5 show the mean value curves obtained from test series 2. These curves show a similar behavior to those in test series 1.

It is obvious that the strength increases considerably with the overlap width up to a width of 10.5 mm, which is shown in Figure 3.6 where the ultimate strengths from test series 1 and 2 are plotted against the corresponding overlap width. After 10.5 mm the increase in strength is very modest and it even decreases between 16.5

and 23 mm, but this is most likely due to the small amount of samples.

The relationship between the overlap width and the strength was approximated with a function as shown in Eq. 3.1. The approximation relates the strength F to the overlap width w as

$$F(w) = a(1 - b^{-w^c}) \tag{3.1}$$

where a describes the horizontal asymptote, b the slope of the curve and c the form of curve. This function was fitted to the experimental data and the values of a, b and c were determined to 205, 1.11 and 1.34 respectively. The approximating function with F in [N] and w in [mm] then looks like

$$F(w) = 205(1 - 1.11^{-w^{1.34}}) \tag{3.2}$$

In Figure 3.6 is the approximating function plotted together with the ultimate strengths from test series 1 and 2.

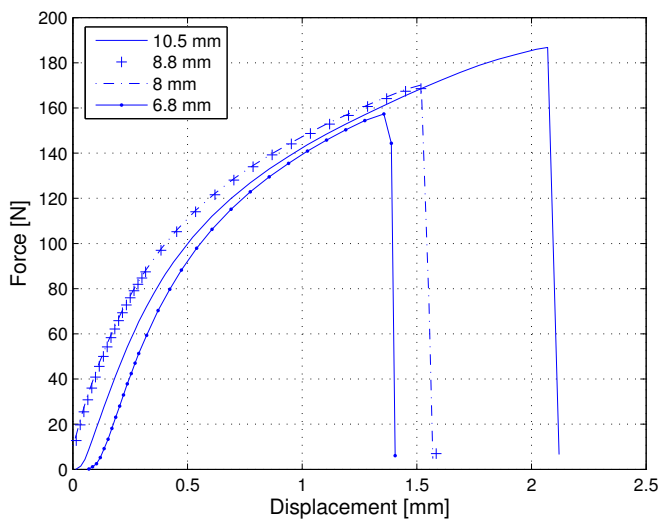

Figure 3.5: *Mean value curves from test series 2.*

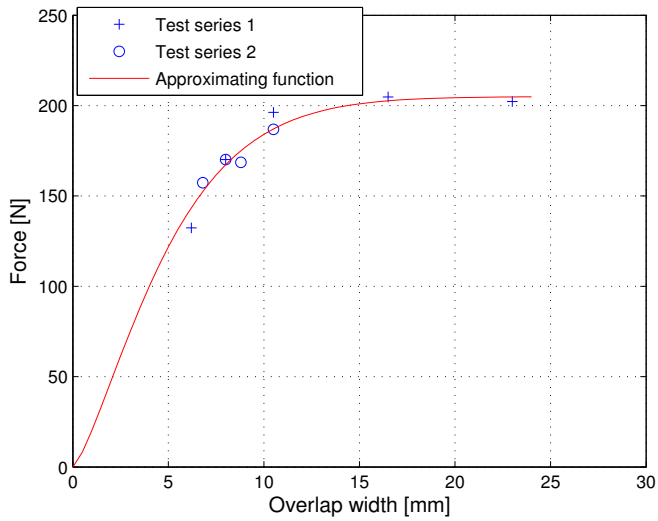

Figure 3.6: *Ultimate strength from test series 1 and 2 and the approximating function*

3.5.3 Test series 3 - folded strip and strip

In Figure 3.7 the results of the tests performed on *folded strip* sealings made in the package rig and a package machine are shown. There seems to be a great deal of difference in strength between the sealings made in these two types of machines. They have similar initial behavior, but the sealings made in the package rig shows a much lower ultimate strength. Probably are the settings for the induction heating somewhat different in the machines.

The specimens with the *strip* sealing taken from the juice packages show a quite differing behavior from the *folded strip* sealings, as presented in Figure 3.8. This is due to the different sealing types and the fact that the juice packages were made of another laminate than the laminate used in this report. The juice packages have also been exposed to i.e moisture which may have affected the laminate.

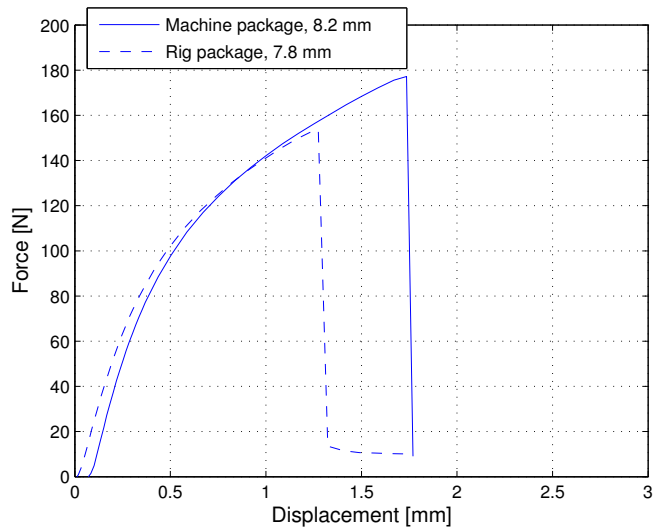

Figure 3.7: *Mean value curves from test series 3 for machine package and rig package (folded strip)*

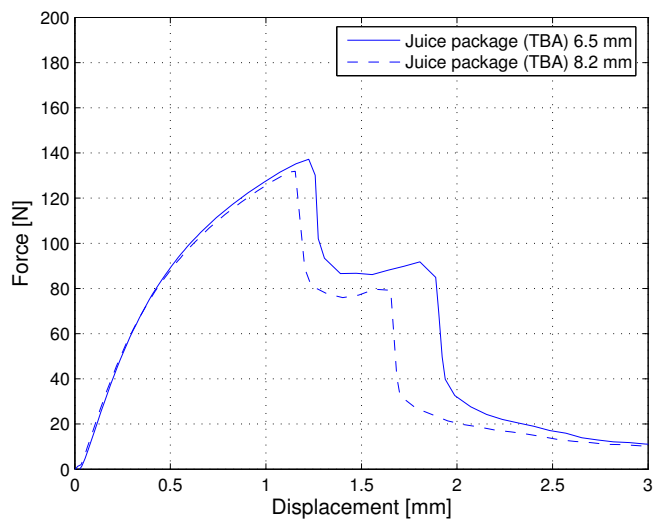

Figure 3.8: *Mean value curves from test series 3 for juice packages (strip)*

3.5.4 Test series 4 - paper orientation

The difference in the behavior of the same samples is quite remarkable when the MD and the CD is oriented in the horizontal length direction respectively. When MD is oriented in the horizontal length direction the sealing shows a much stiffer behavior. The ultimate strength is reached when the displacement is only about 0.8 mm. The difference compared to when the CD is oriented in the horizontal length direction is considerable, where the ultimate strength is reached when the displacement is about 2.1 mm, as shown in Figure 3.9. Though is the mechanical work, which is the area below the curve, approximately 40 % higher for the CD case.

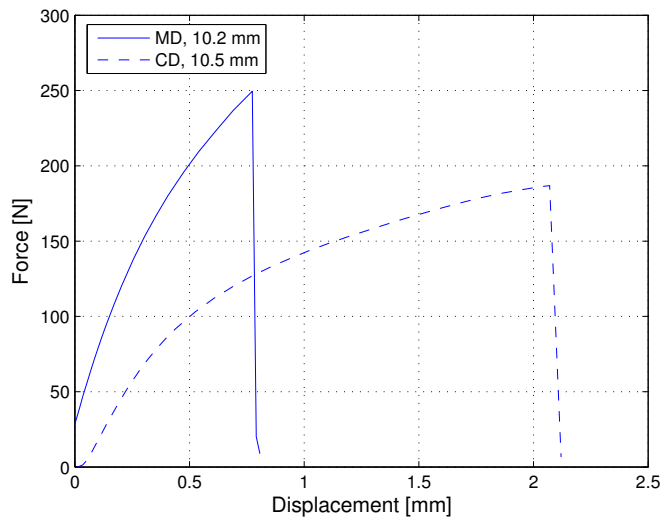

Figure 3.9: *Mean value curves from test series 4*

3.5.5 Test series 5 - unsealed channel

Figure 3.10 shows that a sealing with an unsealed channel have only a slight influence on the ultimate strength. The difference in initial behavior and hardening is negligible.

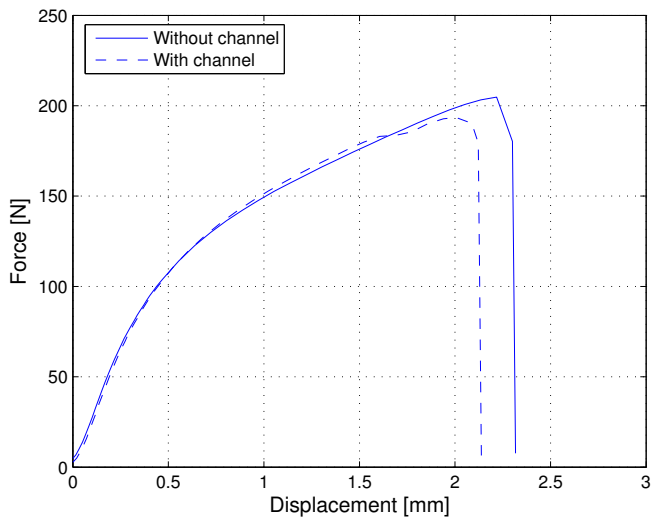

Figure 3.10: *Mean value curves from test series 5*

3.5.6 Test series 6 - laminate

The packaging laminate used in this report shows the same mechanical behavior as the *folded strip* sealing does, as shown in Figure 3.11. This indicates that it is the properties of the laminate that determine the mechanical behavior of the sealing and the geometry of the sealing that determines the ultimate strength.

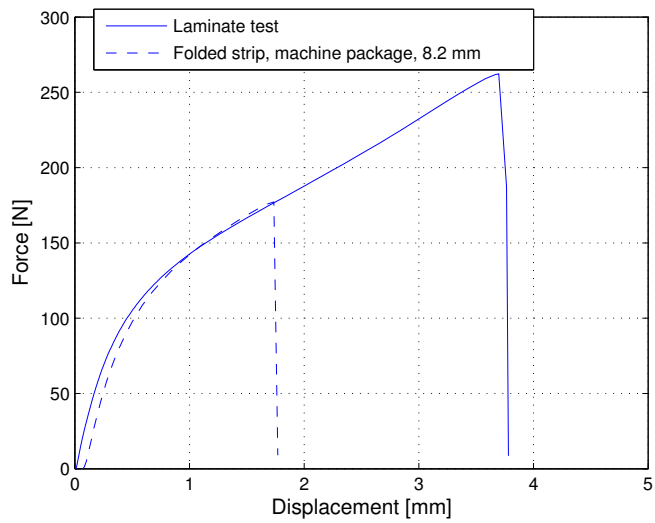

Figure 3.11: *Mean value curve from test series 6 compared to mean value curve from test series 3 (machine package)*

3.6 Discussion on experimental results

The fracture propagations were somewhat different in these tests. The propagation started and proceeded in some cases in the upper laminate, as shown in Figure 3.12 and in other cases in the lower laminate as in Figure 3.13. The propagation proceeded more often in the upper laminate when the overlap width was small. All reasons for this phenomenon are still unknown, but it is partially due to local imperfections in the packaging material. The approximation made on the results from

Figure 3.12: *Fracture propagation in the upper laminate*

Figure 3.13: *Fracture propagation in the lower laminate*

test series 1 and 2 should be considered as a rough guess. It must also be mentioned that it only is valid for the sealing type *no strip*. An approximation which is valid for the sealing types *strip* and *folded strip* ought to have similar behavior but different horizontal asymptote.

The difference in strength between the rig package sealings and the machine package sealings can maybe be explained by the different pressures from the inductor. The rig seemed to put a higher pressure on the package laminate than the machine did, c.f Figure 3.14 and 3.15. The rig package sealing is far more compressed in the upper laminate which maybe could have caused an initial plasticity in the paperboard and by that a decreased ultimate strength.

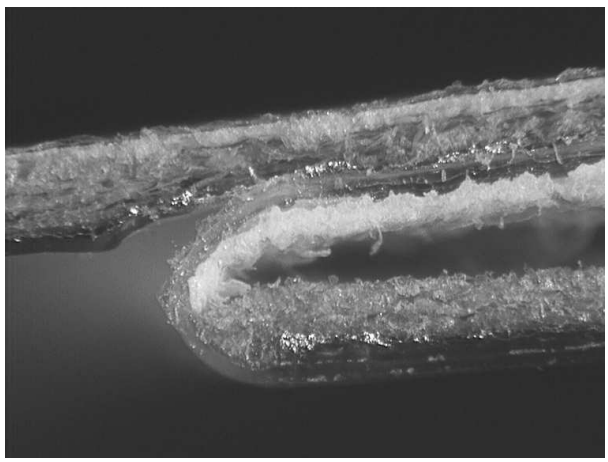

Figure 3.14: *Detail of a specimen made in the rig*

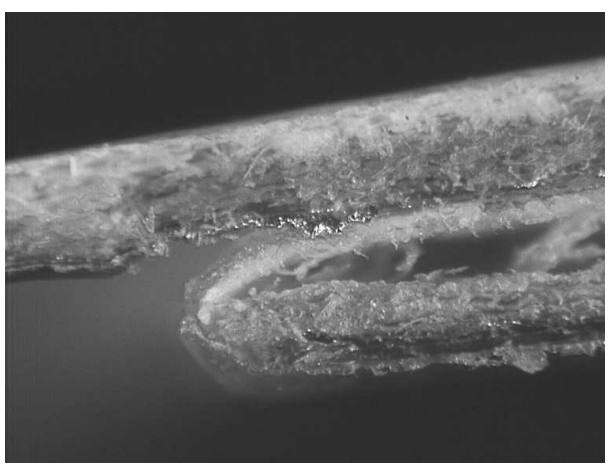

Figure 3.15: *Detail of a specimen made in the machine*

The fact that the pure laminate and the longitudinal sealings show the same mechanical behavior implies that a change of the geometry of the sealing would change the ultimate strength and a change of the properties of the laminate, foremost the paperboard, would change the whole behavior.

Chapter 4

FE-theory and material models

4.1 General remarks

Physical problems are often described with differential equations, which usually are difficult to solve analytically. The Finite Element Method (FEM), is a numerical method used to solve differential equations which are too complex to be solved analytically. Since it is a numerical method it does not give an exact solution. The method is used within several different fields in nature science, where mechanics is one of them. Instead of formulating equations that is valid for the whole region that is studied, the region is divided into a great many parts, which are called finite elements. Approximating equations are then formulated for each element at a time, instead of for the whole region. Dividing the region into elements provide a possibility to do better approximations, i.e it is often enough to assume that each element has a linear behavior even though the whole region shows to have a non-linear behavior. The elements are connected through nodal points. The unknown variable is calculated in each nodal point, whereas the variation within an element is determined through interpolation. A general approach to solve differential problems is presented in Figure 4.1 [6].

The FE-simulations in this study will be accomplished by the FE program ABAQUS 6.5-3. The material model used for paper, the 3DM, is written for ABAQUS as a FORTRAN subroutine and will be described later in this chapter.

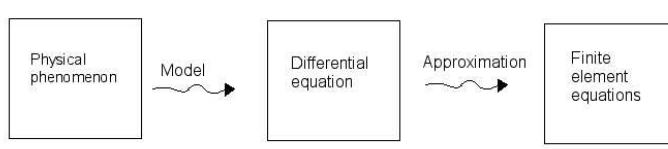

Figure 4.1: *Steps in engineering mechanical analysis [6]*

4.2 Linear elasticity

A package material initially acts according to Hooke' s law, which deals with linear elasticity, when it is loaded. In a one dimension case, Hooke's law is expressed as

$$\sigma = E\epsilon \tag{4.1}$$

where σ is the stress, E is Young's modulus and ϵ is the strain. For the case with two and three dimensions, Hooke's generalized law is given by

$$\sigma = \mathbf{D}\epsilon \tag{4.2}$$

where $\mathbf{D}$ is the constitutive matrix. Assuming plain strain and isotropy, the constitutive matrix is given by

$$\mathbf{D} = \frac{E}{(1+\nu)(1-2\nu]} \begin{bmatrix} 1-\nu & \nu & 0 \\ \nu & 1-\nu & 0 \\ 0 & 0 & \frac{1}{2}(1-2\nu) \end{bmatrix} \tag{4.3}$$

where ν is Poisson´s ratio

For an orthotropic material as paper the constitutive matrix is not quite that simple. The relation is given by

$$\begin{bmatrix} \sigma_{11} \\ \sigma_{22} \\ \sigma_{33} \\ \tau_{12} \\ \tau_{13} \\ \tau_{23} \end{bmatrix} = \begin{bmatrix} D_{11} & D_{12} & D_{13} & 0 & 0 & 0 \\ D_{21} & D_{22} & D_{23} & 0 & 0 & 0 \\ D_{31} & D_{32} & D_{33} & 0 & 0 & 0 \\ 0 & 0 & 0 & D_{44} & 0 & 0 \\ 0 & 0 & 0 & 0 & D_{55} & 0 \\ 0 & 0 & 0 & 0 & 0 & D_{66} \end{bmatrix} \begin{bmatrix} \varepsilon_{11} \\ \varepsilon_{22} \\ \varepsilon_{33} \\ \gamma_{12} \\ \gamma_{13} \\ \gamma_{23} \end{bmatrix} \tag{4.4}$$

where ϵ and γ are normal strains and shear strains respectively, whereas σ and τ are normal stresses and shear stresses respectively. The directions 1,2 and 3 are the same as the directions MD, ZD and CD respectively. In matrix notation, this relation may be written as

$$\boldsymbol{\sigma} = \boldsymbol{D}\boldsymbol{\epsilon} \tag{4.5}$$

An inversion of of this relation gives

$$\boldsymbol{\epsilon} = \boldsymbol{C}\boldsymbol{\sigma} \tag{4.6}$$

where $\boldsymbol{D} = \boldsymbol{C^{-1}}$. The latter expression is necessary when assigning the material properties in ABAQUS. Eq. 4.6 is explicitly given by

$$\begin{bmatrix} \varepsilon_{11} \\ \varepsilon_{22} \\ \varepsilon_{33} \\ \gamma_{12} \\ \gamma_{13} \\ \gamma_{23} \end{bmatrix} = \begin{bmatrix} 1/E_1 & -\nu_{21}/E_2 & -\nu_{31}/E_3 & 0 & 0 & 0 \\ -\nu_{12}/E_1 & 1/E_2 & -\nu_{32}/E_3 & 0 & 0 & 0 \\ -\nu_{13}/E_1 & -\nu_{23}/E_2 & 1/E_3 & 0 & 0 & 0 \\ 0 & 0 & 0 & 1/G_{12} & 0 & 0 \\ 0 & 0 & 0 & 0 & 1/G_{13} & 0 \\ 0 & 0 & 0 & 0 & 0 & 1/G_{23} \end{bmatrix} \begin{bmatrix} \sigma_{11} \\ \sigma_{22} \\ \sigma_{33} \\ \tau_{12} \\ \tau_{13} \\ \tau_{23} \end{bmatrix} \tag{4.7}$$

where E_i is Young's modulus in respective direction and ν_{ij} is Poisson's ratio that describes the transverse strain in j-direction when the material is stressed in i-direction. ν_{ij} and ν_{ji} are related as

$$\frac{\nu_{ij}}{E_i} = \frac{\nu_{ji}}{E_j} \tag{4.8}$$

thus the **C** and **D** matrices are symmetric.

4.3 Plasticity

Plastic strains develop when a material is loaded above its initial yield stress. Even though it is unloaded, plastic strains will remain as shown in Figure 4.2. The behavior is elastic with the stiffness E until the initial yield stress σ_{y0} is reached, after which plastic strains begins to develop if the loading proceeds. If the material is loaded up to point A and then unloaded, it behaves elastically with the stiffness E to point B where the material is completely unloaded. The plastic strains developed due to the loading above the initial yield stress gave the size of ϵ^p If the material

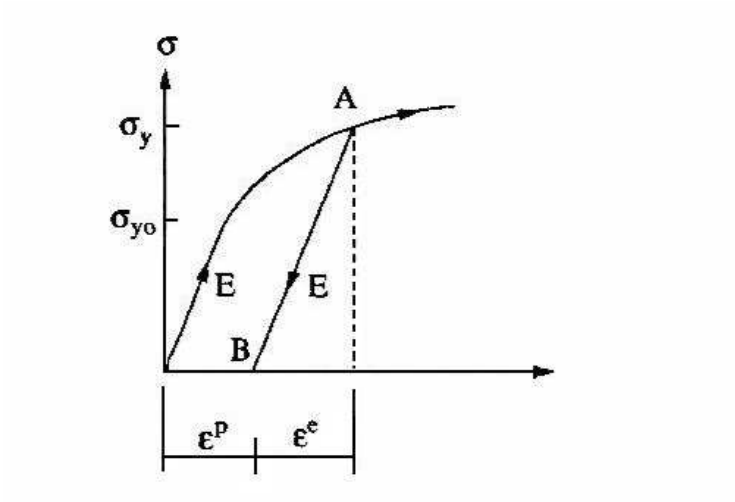

Figure 4.2: *Response of an elasto-plastic material [7]*

is reloaded it will initially behave elastically up to the new yield stress σ_y with the corresponding total strain $\epsilon^e + \epsilon^p$, after which it will respond according to the initial plastic behavior.

In this work is the von Mises plasticity model with isotropic hardening adopted for the LDPE, polymer film and PET material. The paperboard is in the introductory simulations also treated as a material with linear hardening, but the orthotropic

Hill plasticity model is employed, which consider the anisotropy in the paperboard. In the more accurate 3DM simulations is the 3DM in section 4.4 employed.

4.4 The 3DM

A three dimensional material model for orthotropic materials, the 3DM, was first developed by Steve Xia at MIT [9]. It has later on been improved by Ph.D. Mikael Nygårds at STFI-Packforsk, Ph.D. Johan Tryding at Tetra Pak and Lund Institute of Technology in cooperation, among others. Since paperboard consists of several layers within a board as shown in Figure 4.3, it is necessary to have two different models describing the behavior of the material. The continuum model describes the material behavior of the layers and the interface model describes the material behavior in fracture between the layers, which is shown in Figure 4.4. Here a brief discussion of the 3DM and its material parameters are presented. For a more detailed presentation of the 3DM, see Xia [9] and Nygårds [5].

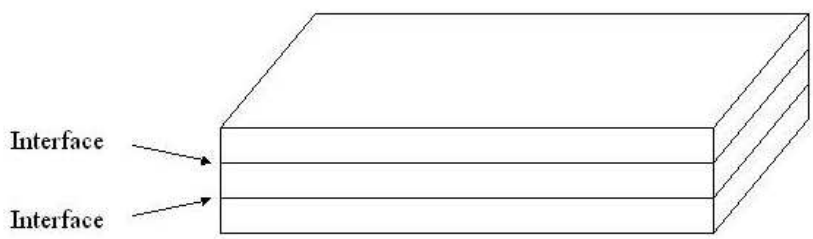

Figure 4.3: *Layers in paperboard*

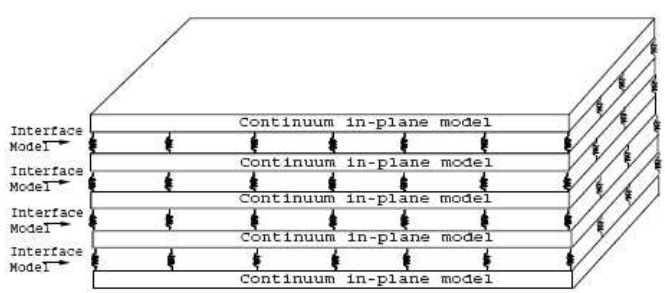

Figure 4.4: *Continuum model and interface model [9].*

4.4.1 Continuum model

The continuum model UMAT, implemented in ABAQUS as a user material routine, explains the material behavior within one paper layer. In the model it is presumed that plasticity only occurs in the MD-CD plane. In the input file submitted to ABAQUS, the material properties of the paperboard should be specified in an input deck as

∗MATERIAL,NAME=paper
∗USER MATERIAL,TYPE=MECHANICAL,CONSTANTS=44,UNSYMM

E_{MD},	E_{ZD},	E_{CD},	ν_{ZDMD},	ν_{MDCD},	ν_{ZDCD},	G_{MDZD},	G_{MDCD}
G_{ZDCD},	ϕ,	a,	b,	c,	$2k$,	S_0^1,	S_0^2
S_0^3,	S_0^4,	S_0^5,	A_1,	A_2,	A_3,	A_4,	A_5
B_1,	B_2,	B_3,	B_4,	B_5,	C_1,	C_2,	C_3
C_4,	C_5,	N^1_{MDMD},	N^1_{CDCD},	N^2_{MDMD},	N^2_{CDCD},	N^3_{MDCD},	N^4_{MDMD}
N^4_{CDCD},	N^5_{MDMD},	N^5_{CDCD},	N^6_{MDCD}				

∗DEPVAR

The first row and the first parameter in the second row specifies the engineering constants described in the lower matrix in Eq. 4.7. E_{MD}, E_{ZD} and E_{CD} are the elastic modulus in each direction respectively. ν_{ZDMD} and ν_{ZDCD} are the out-of-plane Poisson's ratio whereas ν_{MDCD} is the in-plane Poisson's ratio. G_{MDZD} and G_{ZDCD} are the out-of-plane shear modulus and G_{MDCD} is the in-plane shear modulus. ϕ is the angle between MD and the global axis. The material constants a, b and c are parameters in exponential functions that describes the elastic modulus E_{ZD} and the shear modulus G_{MDZD} and G_{ZDCD} for compression in ZD ($E_{ZDZD} < 0$). The behavior in compression is nonlinear elastic and described as

$$E_{ZD} = E^0_{ZD} e^{-aE^e_{ZDZD}} \tag{4.9}$$

$$G_{MDZD} = G^0_{MDZD} e^{-bE^e_{ZDZD}} \tag{4.10}$$

$$G_{ZDCD} = G^0_{ZDCD} e^{-cE^e_{ZDZD}} \tag{4.11}$$

It is in the continuum model assumed that the yield surface can be created by n subsurfaces, where N^I is normal to the I:th subsurface. In the 3DM code n usually equals six, and the subsurfaces and gradients then looks as in Figure 4.5. It is below presumed that n equals six.

The N-vectors describes in which direction the material should continue to yield. The yielding function f is expressed by

$$f(\bar{\mathbf{T}}, \bar{\gamma}) = \sum_{I=1}^{n} \chi_I \left(\frac{\bar{\mathbf{T}} : \mathbf{N^I}}{S^I(\bar{\gamma})}\right)^{2k} - 1 \tag{4.12}$$

where $\bar{\mathbf{T}}$ is the second Piola-Kirchoff stress, $\bar{\gamma}$ is the equivalent plastic strain, $2k$ is an exponent, $S^I(\bar{\gamma})$ are the equivalent strengths for each subsurface respectively and

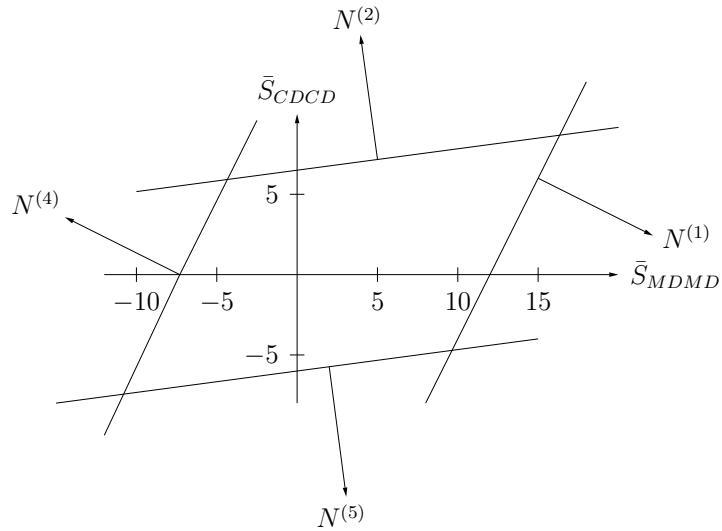

Figure 4.5: The yield planes and gradients when $\bar{S}_{MDCD} = 0$. [4]

χ_I is given as

$$\chi_I = \begin{cases} 1 & if \quad \bar{\mathbf{T}} : \mathbf{N^I} > 0; \\ 0 & otherwise \end{cases} \tag{4.13}$$

Further on is S_0^1 the initial tensile yield stress in MD, S_0^2 is the initial tensile yield stress in CD, S_0^3 is the initial yield stress in shear, S_0^4 is the initial compression yield stress in MD and S_0^5 is the initial compression yield stress in CD. A_1 to C_5 are hardening parameters affecting the equivalent strengths as shown in Eq. 4.14 to 4.19.

$$S^1(\bar{\gamma}) = S_0^1 + A_1 tanh(B_1\bar{\gamma}) + C_1\bar{\gamma} \quad (4.14)$$
$$S^2(\bar{\gamma}) = S_0^2 + A_2 tanh(B_2\bar{\gamma}) + C_2\bar{\gamma} \quad (4.15)$$
$$S^3(\bar{\gamma}) = S_0^3 + A_3 tanh(B_3\bar{\gamma}) + C_3\bar{\gamma} \quad (4.16)$$
$$S^4(\bar{\gamma}) = S_0^4 + A_4 tanh(B_4\bar{\gamma}) + C_4\bar{\gamma} \quad (4.17)$$
$$S^5(\bar{\gamma}) = S_0^5 + A_5 tanh(B_5\bar{\gamma}) + C_5\bar{\gamma} \quad (4.18)$$
$$S^6(\bar{\gamma}) = S^3 \quad (4.19)$$

The ten N-parameters are gradients to the six vectors describing the yield planes. The values of the gradients are given in Table 4.1.

Table 4.1: Components of the gradients N^α

α	N^α_{MDMD}	N^α_{CDCD}	N^α_{MDCD}	
1	$2/\sqrt{5}$	$-1/\sqrt{5}$	0	MD tension
2	$-2/\sqrt{229}$	$15/\sqrt{229}$	0	CD tension
3	0	0	$\sqrt{2}/2$	Shear
4	$-2/\sqrt{5}$	$1/\sqrt{5}$	0	MD compression
5	$2/\sqrt{229}$	$-15/\sqrt{229}$	0	CD compression
6	0	0	$-\sqrt{2}/2$	Shear

4.4.2 Interface model

The interface model UINTER, implemented in ABAQUS as a user interface, characterizes the behavior between two surfaces and is primarily intended to be used to model delamination. In the input file, the properties of the interfaces should be specified as

∗ SURFACE INTERACTION,NAME=inter1,USER, DEPVAR=20, PROPERTIES=15, UNSYMM
thickness
K^0_{MD}, K^0_{ZD}, S^0_{MD}, S^0_{ZD}, K^0_{CD}, S^0_{CD}, A, B,
C, R^{ZD}_s, R^{MD}_s, R^{CD}_s, R^{ZD}_k, R^{MD}_k, R^{CD}_k

where the parameter *thickness* is the out-of-plane thickness for two-dimensional models. For three-dimensional models is a blank line inserted instead. K^0_{MD} is the initial shear stiffness in MD direction, K^0_{ZD} is the initial stiffness in tension in ZD, S^0_{MD} is the initial yield stress in MD shear and S^0_{ZD} is the initial yield stress in tension in ZD. Further on is K^0_{CD} the initial shear stiffness in CD and S^0_{CD} is the initial shear stiffness in CD. To explain the remaining parameters, a more detailed discussion is done below.

The interface damage parameter D describes how the interface is damaged and is given by

$$D(\bar{\delta}^p) = tanh(\frac{\bar{\delta}^p}{C}) \tag{4.20}$$

where $\bar{\delta}^p$ is the equivalent plastic displacement. The interface damage affects the instantaneous stiffness K, which in the α -direction is characterized as

$$K_\alpha(\bar{\delta}^p) = K_\alpha^0(1 - R_\alpha^k D(\bar{\delta}^p)) \tag{4.21}$$

Both the material constants C and R_α^k does in other words affect the instantaneous stiffness i.e the stiffness in every time increment. R_{ZD}^k and R_{ZD}^s are the residual strength factor in ZD, determining how fast the material is getting softer. Likewise are R_{MD}^k, R_{MD}^s, R_{ZD}^k and R_{ZD}^s the residual shear strength factor in each direction respectively. The instantaneous interface strength S is also affected by these parameters in the same manner as shown in Eq. 4.22.

$$S_\alpha(\bar{\delta}^p) = S_\alpha^0(1 - R_\alpha^k D(\bar{\delta}^p)) \tag{4.22}$$

The relationship between the instantaneous strength S_α, the instantaneous stiffness K_α and the interface damage is shown in Figure 4.6.

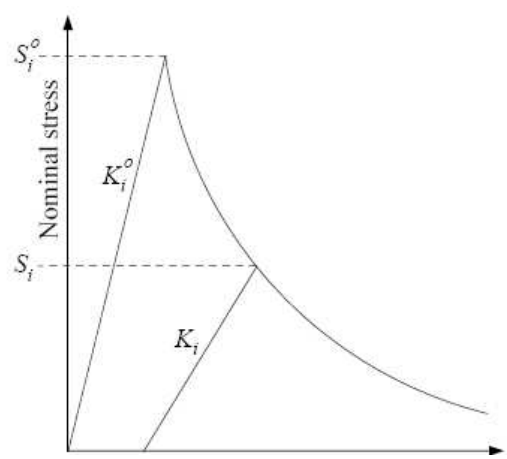

Figure 4.6: *Relationship between stress, stiffness and interface displacement [5]*

The yielding criterion f is given by

$$f(T, \bar{\delta}^p) = \sum_{\alpha=2}^{n} \frac{S_1 T_\alpha^2}{S_\alpha(\bar{\delta}^p)^2} + T_1 - S_1 \tag{4.23}$$

where T is a traction vector containing the forces acting on an infinitesimal area on a boundary. Yielding occurs in the interfaces when the yielding criterion function equals zero.

A and B are material constants affecting the plastic flow direction, which after initial yielding determines in which direction the material should continue to yield. The plastic flow rule is governed by

$$\Delta\delta_i^p = \chi M_i \Delta\bar{\delta}^p \tag{4.24}$$

where M_i are the components of the unit flow and χ is either zero or one, depending on the yield criterion. For non-associated flow, as in this case, the plastic flow is given by

$$\hat{M}_1 = \mu(\bar{\delta}^p)\frac{\partial f}{\partial T_1} = \mu(\bar{\delta}^p) \tag{4.25}$$

$$\hat{M}_\alpha = \frac{\partial f}{\partial T_\alpha} = 2\frac{S_1(\bar{\delta}^p)}{S_1(\bar{\delta}^p)^2}T_\alpha \quad \alpha = 2,3 \tag{4.26}$$

where μ is a frictional function that depends on the equivalent plastic displacement and the material constants A and B. It is described as

$$\mu = A(1 - BD(\bar{\delta}^p)) \tag{4.27}$$

4.4.3 Transformation of input data for the 3DM model

Since the 3DM routine is written for the cases of creasing and folding operations, the MD is in the FORTRAN implementation oriented in the 1-direction. Unfortunately it is in ABAQUS not possible to transform the material directions in a two dimensional model in such manner that the CD is oriented in the 1-direction, which is the case for this study. Hence, it was a matter of necessity to transform the input properties for UMAT and UINTER in order to make it valid for this study. Because of the the symmetry in the **D** matrix in Eq. 4.7, not all parameters are given in the matrix. When changing the material direction other Poisson's ratios were needed to be calculated, which was accomplished by using Eq. 4.8.

The main task was to transform the input parameters in UMAT and UINTER in such a manner that the CD became the 1-direction, which makes it necessary to change places of E_{MD} and E_{CD} in the input deck in UMAT. Further on ν_{ZDMD} changes place with ν_{ZDCD} and ν_{CDMD} needs to be calculated according to Eq. 4.8. The shear modulus G_{MDZD} changes place with G_{ZDCD} (which is the same as G_{CDZD}). The parameters ϕ, a and $2k$ are unchanged, whereas b and c change places with each other, according to Eq. 4.9 to 4.11. The new directions of the vectors N^α are shown in Figure 4.7. This figure can be compared with the old gradients presented in Figure 4.5 to easier see the transformation.

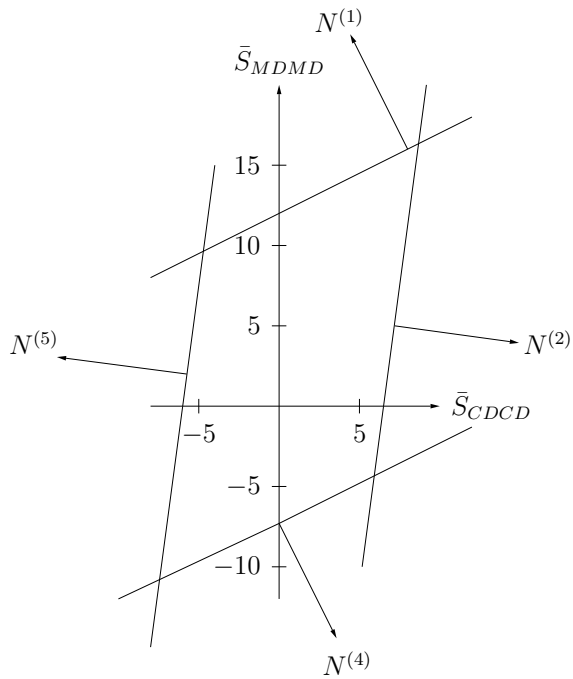

Figure 4.7: The transformed yield planes and gradients when $\bar{S}_{MDCD} = 0$

The gradients N^1 and N^2 will change places as well as N^4 and N^5, whereas N^3 and N^6 are unchanged. Since the vectors are two gradients, it is also necessary to change place of N^{α}_{MDMD} and N^{α}_{CDCD}. The yield stresses S_0 change places in the same manner, i.e yield stresses with index 1 and 2 changes place with index 4 and 5 respectively whereas 3 and 6 does not move. The hardening parameters A_1 to C_5 moves in the same manner as the yield stresses according to Eq. 4.14 to 4.19. The original configuration of the input deck in UMAT as well as the new configuration with CD in 1-direction are shown below.

∗MATERIAL,NAME=paperMD1
∗USER MATERIAL,TYPE=MECHANICAL,CONSTANTS=44,UNSYMM
E_{MD}, E_{ZD}, E_{CD}, ν_{ZDMD}, ν_{MDCD}, ν_{ZDCD}, G_{MDZD}, G_{MDCD}
G_{ZDCD}, ϕ, a, b, c, $2k$, S_0^1, S_0^2
S_0^3, S_0^4, S_0^5, A_1, A_2, A_3, A_4, A_5
B_1, B_2, B_3, B_4, B_5, C_1, C_2, C_3
C_4, C_5, N^1_{MDMD}, N^1_{CDCD}, N^2_{MDMD}, N^2_{CDCD}, N^3_{MDCD}, N^4_{MDMD}
N^4_{CDCD}, N^5_{MDMD}, N^5_{CDCD}, N^6_{MDCD}
∗DEPVAR

∗ MATERIAL,NAME=paperCD1
∗ USER MATERIAL,TYPE=MECHANICAL,CONSTANTS=44,UNSYMM
E_{CD}, E_{ZD}, E_{MD}, ν_{ZDCD}, ν_{CDMD}, ν_{ZDMD}, G_{CDZD}, G_{CDMD}
G_{ZDMD}, ϕ, a, c, b, $2K$, S_0^2, S_0^1
S_0^3, S_0^5, S_0^4, A_2, A_1, A_3, A_5, A_4
B_2, B_1, B_3, B_5, B_4, C_2, C_1, C_3
C_5, C_4, N^2_{CDCD}, N^2_{MDMD}, N^1_{CDCD}, N^1_{MDMD}, N^3_{MDCD}, N^5_{CDCD}
N^5_{MDMD}, N^4_{CDCD}, N^4_{MDMD}, N^6_{MDCD}
∗ DEPVAR

The same routine is used to change the parameters in the interface model, i.e parameters with index MD changes place with index CD. The material constants A,B and C are unchanged. The original input deck in UINTER as well as the new with CD in 1-direction are shown below.

∗ SURFACE INTERACTION,NAME=interMD1,USER, DEPVAR=20, PROPERTIES=15, UNSYMM
thickness
K^0_{MD}, K^0_{ZD}, S^0_{MD}, S^0_{ZD}, K^0_{CD}, S^0_{CD}, A, B,
C, R_s^{ZD}, R_s^{MD}, R_s^{CD}, R_k^{ZD}, R_k^{MD}, R_k^{CD}

∗ SURFACE INTERACTION,NAME=interCD1,USER, DEPVAR=20, PROPERTIES=15, UNSYMM
thickness
K^0_{CD}, K^0_{ZD}, S^0_{CD}, S^0_{ZD}, K^0_{MD}, S^0_{MD}, A, B,
C, R_s^{ZD}, R_s^{CD}, R_s^{MD}, R_k^{ZD}, R_k^{CD}, R_k^{MD}

To verify that the changes were valid, a simple three dimensional model consisting only of a few paper elements was built up in ABAQUS. The model was loaded in the CD with ordinary material properties and in the CD with new material properties. The model was set to be fully constrained in all directions except the loading direction, where it was subjected to a displacement of totally 1 mm. Results from these simulations are plotted in Figure 4.8. The two curves follow each other exactly, so it is assumed that the changed material model gives identical results with the original material model.

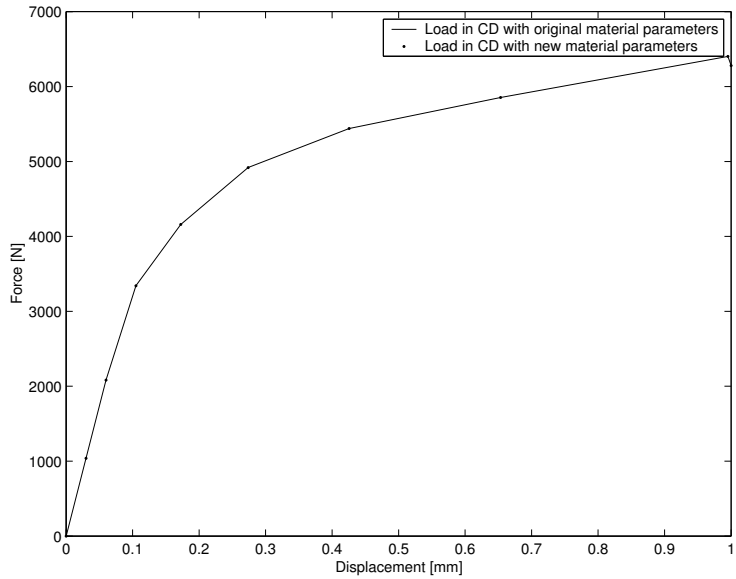

Figure 4.8: *Force-displacement diagram to verify changes*

Chapter 5

FE-modelling

5.1 Introduction

FE-simulations of the various sealings in section 2.4 were made with the aim of predicting the behavior and the ultimate strength of the sealings. The simulations were performed with the computer simulation program ABAQUS [1], which is a general purpose program when it comes to finite element problems, both linear and nonlinear. ABAQUS has a comprehensive library of elements and material models for various applications, which gives the user freedom to model a wide range of geometries and engineering materials. The two main solvers in the program are ABAQUS/Standard and ABAQUS/Explicit. ABAQUS/Standard is a general analysis product which uses implicit time integration. It is a good solver when analyzing static, dynamic, thermal and electrical problems, both linear and nonlinear geometries and materials. The 3DM model is written for implicit time integration, hence is ABAQUS/standard used in this work. ABAQUS/Explicit is a special-purpose analysis module. It uses explicit dynamic time integration suitable for transient dynamic and highly non-linear problems.

The 3DM routine is written as a FORTRAN subroutine that is linked with ABAQUS during run-time. An analysis with user defined material is executed at the command prompt by the command

abaqus job=inputfilename user=subroutinename.f

Depending on the operative system on the computer, the file ending may be ∗.for instead. Generally ∗.for is used in Windows and ∗.f in Unix and Linux. For the case where the inputfile name is nostrip.inp and the name of the FORTRAN subroutine is 3dm32.f the command looks like

abaqus job=nostrip user=3dm32.f

If several subroutines are used, they need to be in the same file. The subroutine 3dm32.f contains for instance the subroutine for the continuum model, presented in section 4.4.1 and the subroutine for the interface model presented in section 4.4.2 [5].

5.2 Modelling procedures

The modelling is preferably done in a graphical environment called Complete ABAQUS Environment (CAE). The geoemtry can either be built by parts in the CAE or imported from a CAD program. The parts are defined in the parts module and then assembled into a model in the assembly module and assigned material properties in the property module. The different load steps that are needed are defined in the step module and the interactions (the interfaces) are defined in the interaction module. The boundary conditions and loads are defined in the load module. After this, the model is meshed in the mesh module. An input file containing the geometry, boundary conditions, material properties etc. is created after meshing. The user defined material and interaction properties are then added to the input file, since that is not possible to do in the CAE [1].

When creating the model it is of great advantage to use a convenient naming convention for the various parts, materials, sets etc., see Appendix C. It is much easier to debug the input file when a naming convention is used.

The *no strip* model was built from five various parts. One part for the chemical and mechanical paper respectively, one part for the LDPE on the top and two parts consisting of LDPE, aluminum and polymer film. The parts are presented in Figure 5.1. To the other models was a strip added and therefore they are built from six various parts.

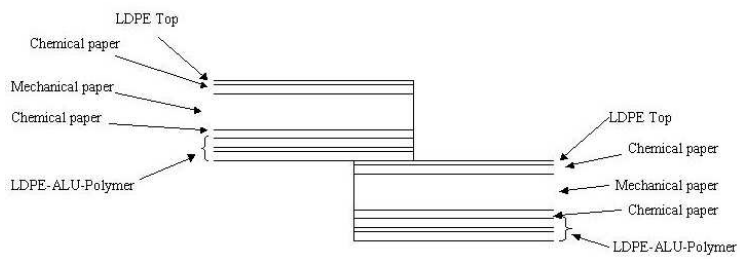

Figure 5.1: *The five parts in the no strip model (not made to scale).*

5.3 Geometry

In order to imitate the experimental setup as much as possible, the test specimens in section 3.2 were modelled with a length of 50 mm, a thickness of 0.482 mm and a depth of 15 mm as shown in Figure 5.2. When one model was built, it was quite easy to build the other models by copying the first model and modifying the overlap width and the thickness of the paperboard.

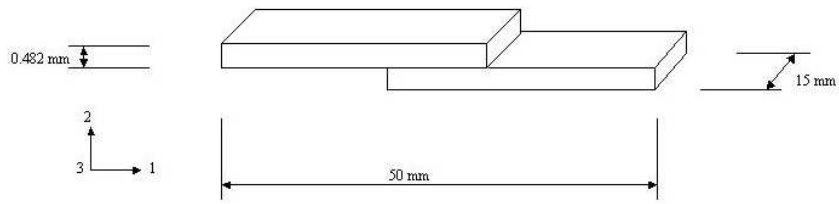

Figure 5.2: *Geometry*

The sealings were simulated in two dimensions to minimize the number of elements. The elements used in this simulation were two-dimensional, 4-node, plane strain, quadrilateral solid elements called CPE4 in ABAQUS/Standard. A finer mesh was established around the sealing to get a higher accuracy where large stress gradients was expected. The aim was to produce a mesh with at least two elements for each material in the thickness direction. Since it is desirable to have as square shaped elements as possible, the number of elements became rather large due to large number of layers in the packaging material. An average model consists of approximately 100 000 elements.

5.4 Boundary conditions

Boundary conditions were applied on the both short edges of the model shown in Figure 5.2. A displacement was prescribed in the horizontal 1-direction at the right edge, whereas the rotation around the three-direction out of the model was fixed. The left edge was fully constrained. The simulations were displacement controlled since a more stable solution usually is obtained for a non-linear simulation with fracture.

5.5 Introductory simulations

Introductory simulations were made in order to investigate what types of material models that are needed in these types of simulations.

5.5.1 Material properties for introductory simulations

All materials were modelled as elastic-plastic materials, thus they behave elastic until the yield stress is reached, after which the linear hardening begins. The elastic input material data for all materials except paper is given in Table 5.1 and the plastic material data is given in Table 5.2. All data presented in this section are proposals from Andreasson (2005). Aluminum, LDPE and the polymer film was modelled according to von Mises plasticity with isotropic linear hardening. The magnitude

of the hardening (the slope of the plastic part of the curve) is determined by the plastic strain ϵ^p and the corresponding stress.

The paper was assumed to follow the orthotropic Hill plasticity model, which may be used when modelling paper. The elastic parameters employed are shown in Table 5.3. The parameters are termed engineering constants in ABAQUS and define the elastic matrix according to Eq. 4.7. Even though the paperboard consists of three plies, two plies with chemical paper and one with mechanical paper, it is in this model assumed that the board consists of one ply only with a stiffness that lies between the stiffness of the chemical plies and the mechanical ply. The plastic parameters for yielding in CD are given in Table 5.4.

Table 5.1: Elastic material properties

	E [MPa]	ν [-]
Aluminum	70 000	0.30
LDPE	150	0.30
Polymer film	300	0.35

Table 5.2: Plastic material properties

	Stress, σ [MPa]	*Plastic strain,* ϵ^p [-]
Aluminum	50	0
	80	0.0193
LDPE	9	0
	10	0.002
	11	1
Polymer film	18	0
	20	0.002
	22	1

Table 5.3: Elastic material properties of paper.

E_{CD} [MPa]	E_{ZD} [MPa]	ν_{CDZD}	ν_{CDMD}	ν_{ZDMD}	G_{CDZD} [MPa]	G_{CDMD} [MPa]	G_{ZDMD} [MPa]
3000	10	0.5	0.35	0.01	120	1700	85

Table 5.4: Plastic material properties of paper in CD

	Stress σ^0 [MPa]	*Plastic strain* [-]
Paper	40	0
	67	0.0053
	80	0.024

To model the anisotropy, a set of yield ratios must be given (c.f Table 5.5), to determine the actual stress in the various directions. The relationship between the stress and the corresponding ratio is given by

$$\sigma_{ij} = \sigma^0 R_{ij} \tag{5.1}$$

Table 5.5: Yield ratios

R_{CDCD}	R_{ZDZD}	R_{MDMD}	R_{CDZD}	R_{CDMD}	R_{ZDMD}
1	0.015	0.015	0.2	0.2	2

5.5.2 Results of introductory simulations

The result presented in Figure 5.3 is not reliable, such deformed and stretched elements are not similar to the physical behavior in the experimental tests. Paperboard can not stretch as much in the thickness direction ZD as it does in this simulation, at least not without beginning to delaminate. In these quite simple simulations it is shown that the sealing is not the weak region. The delamination in the paperboard is initiated by shearing and when the sealing begins to distort, stresses develop in the ZD with an accompanying fracture propagation.

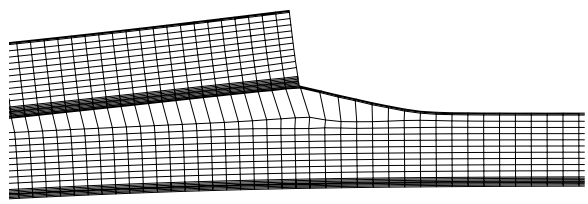

Figure 5.3: *The deformed shape of the introductory model*

In Figure 5.4 are force - displacement curves plotted for the sealing types *no strip*, *strip* and *folded strip*. The ultimate strength for *folded strip* is for some reason considerably lower than for *strip*.

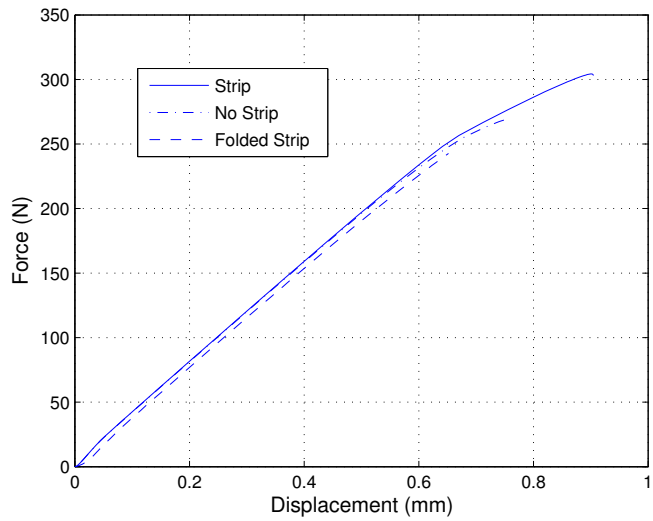

Figure 5.4: *Force - displacement diagram for introductory simulations*

In order to cover the phenomenon of delamination and predict the behavior of paper better, a more detailed model must be implemented. This can be done by i.e nonlinear springs, cohesive elements or the interface model in 3DM. In this work the 3DM was chosen, not only to model delamination, but also to investigate if the 3DM works for other load cases than folding and creasing.

5.6 3DM simulations

In all simulations made after the introductory simulations, the 3DM routine was employed and models were built for all four sealing setups. As mentioned earlier, paperboard is built up by one inner mechanical ply and two outer chemical plies. There are interfaces included between the plies and within the plies,which is shown in Figure 5.5.

In every ply there are three interfaces implemented, which makes it possible for cracks to develop within a ply. Three interfaces within a ply gives according to Elison and Hansson [4] a fair solution. Since the material properties given in Nygårds [5] were aimed to a model with less interfaces, the increased number of interfaces gives a weaker laminate. Hence the initial stiffness K^0_{CD}, K^0_{ZD} and K^0_{MD}, described

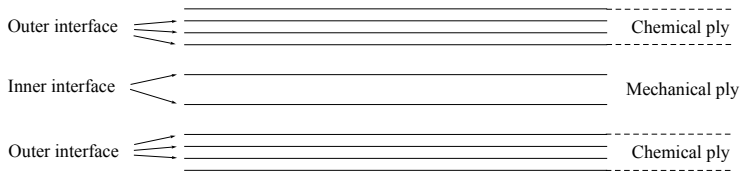

Figure 5.5: *Interfaces in the model [4]*

in section 4.4.2 are increased in the numerical studies.

There are two different types of interfaces acting in the model, the outer interface in the chemical ply and between the mechanical and chemical plies and the inner interface acting in the mechanical ply. Interface properties only exists for the interface in the mechanical ply and between the mechanical and chemical plies. Therefore is it assumed that the properties for the interface between the mechanical and the chemical plies are similar to those in the chemical plies [4].

The various overlap widths for each sealing type simulated are shown in Table 5.6. The *folded strip* model is simulated with an overlap width of 9 mm because that is the width most often used for this sealing type.

Table 5.6: Overlap widths

Sealing type	*Overlap widths* [mm]
No strip	10
Strip	10
Folded strip	9
Edge to edge	10

5.6.1 Material properties in the 3DM simulations

The material properties for aluminum, LDPE and polymer film are given in Table 5.1 and 5.2. The material properties of the elastic part of the paper in the continuum model are given in Table 5.7 and the properties of the plastic part are given in Table 5.8. The material properties for the interface model are given in Table 5.9. All properties are taken directly from Nygårds [5]. In the model with the sealing type *edge to edge*, the strip is made of PET material. This polymer is quite strong an does have an elastic modulus that is close to that of paper. The PET is modelled with von Mises model with linear isotropic hardening. In Table 5.10 are the material properties for the PET shown.

In order to get a more uniform stress distribution, it is desirable to have a strip with approximately the same elastic modulus as the paperboard. To get a rough estimate about a suitable thickness of the strip, the elastic modulus of the paperboard was calculated as the mean value of all elastic modulus in CD of each layer, in relation to their thickness as

$$E_{pb} * (t_{chem} + t_{mech}) = E_{CD}^{chem} * t_{chem} + E_{CD}^{mech} * t_{mech} \tag{5.2}$$

With values inserted from Table 5.7, the elastic modulus of the paperboard becomes $790MN/mm$. Divided by the elastic modulus of the PET material from Table 5.10, the total thickness of the strip becomes approximately $226\mu m$, hence the strip is modelled with a thickness of $100\mu m$ on each side of the laminate.

Table 5.7: Elastic material properties for paper in the continuum model [5].

Notation	*Description*	*Chemical*	*Mechanical*
E_{MD}	Elastic modulus in MD, c.f section 4.4.1	8.9 GPa	3.4 GPa
E_{ZD}	Elastic modulus in ZD, c.f section 4.4.1	25 MPa	16 MPa
E_{CD}	Elastic modulus in CD, c.f section 4.4.1	3.4 GPa	0.96 GPa
ν_{ZDMD}	Out-of-plane Poisson's ratio, c.f section 4.4.1	0.0	0.0
ν_{MDCD}	In-plane Poisson's ratio, c.f section 4.4.1	0.37	0.37
ν_{ZDCD}	Out-of-plane Poisson's ratio, c.f section 4.4.1	0.0	0.0
G_{MDZD}	Out-of-plane shear modulus, c.f section 4.4.1	58.0 MPa	20.0 MPa
G_{MDCD}	In-plane shear modulus, c.f section 4.4.1	2.4 GPa	0.8 GPa
G_{ZDCD}	Out-of-plane shear modulus, c.f section 4.4.1	38.0 MPa	15.0 MPa
ϕ	Angle between MD and global axis	0.0	0.0
a	Exponent in penalty function, c.f Eq. 4.9	5.4	5.4
b	Exponent in penalty function, c.f Eq. 4.10	1.5	1.5
c	Exponent in penalty function, c.f Eq. 4.11	1.5	1.5

Table 5.8: Plastic material properties for paper in the continuum model [5].

Notation	*Description*	*Chemical*	*Mechanical*
2k	Exponent in yield condition, c.f Section. 4.4.1	4	4
S_0^1	Tensile yield stress in MD, c.f Section. 4.4.1	22.0 MPa	10.7 MPa
S_0^2	Tensile yield stress in CD, c.f Section. 4.4.1	16.5 MPa	6.5 MPa
S_0^3	Yield stress in shear, c.f Section. 4.4.1	8.0 MPa	6.0 MPa
S_0^4	Compression yield stress in MD, c.f Section. 4.4.1	6.3 MPa	6.3 MPa
S_0^5	Compression yield stress in CD, c.f Section. 4.4.1	6.3 MPa	6.3 MPa
A_1	Hardening parameter, c.f Eq. 4.14	44.0 MPa	19.0 MPa
A_2	Hardening parameter, c.f Eq. 4.15	7.4 MPa	7.4 MPa
A_3	Hardening parameter, c.f Eq. 4.16	18.0 MPa	7.5 MPa
A_4	Hardening parameter, c.f Eq. 4.17	12.0 MPa	6.0 MPa
A_5	Hardening parameter, c.f Eq. 4.18	12.5 MPa	9.0 MPa
B_1	Hardening parameter, c.f Eq. 4.14	260.0 MPa	260.0 MPa
B_2	Hardening parameter, c.f Eq. 4.15	160.0 MPa	160.0 MPa
B_3	Hardening parameter, c.f Eq. 4.16	375.0 MPa	375.0 MPa
B_4	Hardening parameter, c.f Eq. 4.17	160.0 MPa	160.0 MPa
B_5	Hardening parameter, c.f Eq. 4.18	310.0 MPa	310.0 MPa
C_1	Hardening parameter, c.f Eq. 4.14	800.0 MPa	800.0 MPa
C_2	Hardening parameter, c.f Eq. 4.15	160.0 MPa	160.0 MPa
C_3	Hardening parameter, c.f Eq. 4.16	200.0 MPa	200.0 MPa
C_4	Hardening parameter, c.f Eq. 4.17	300.0 MPa	300.0 MPa
C_5	Hardening parameter, c.f Eq. 4.18	225.0 MPa	225.0 MPa
N^1_{MDMD}	MD tension, c.f Figure 4.5	$2/\sqrt{5}$	$2/\sqrt{5}$
N^1_{CDCD}	MD tension, c.f Figure 4.5	$-1/\sqrt{5}$	$-1/\sqrt{5}$
N^2_{MDMD}	CD tension, c.f Figure 4.5	$-2/\sqrt{229}$	$-2/\sqrt{229}$
N^2_{CDCD}	CD tension, c.f Figure 4.5	$15/\sqrt{229}$	$15/\sqrt{229}$
N^3_{MDCD}	Shear, c.f Figure 4.5	$\sqrt{2}/2$	$\sqrt{2}/2$
N^4_{MDMD}	MD compression, c.f Figure 4.5	$-2/\sqrt{5}$	$-2/\sqrt{5}$
N^4_{CDCD}	MD compression, c.f Figure 4.5	$1/\sqrt{5}$	$1/\sqrt{5}$
N^5_{MDMD}	CD compression, c.f Figure 4.5	$2/\sqrt{229}$	$2/\sqrt{229}$
N^5_{CDCD}	CD compression, c.f Figure 4.5	$-15/\sqrt{229}$	$-15/\sqrt{229}$
N^6_{MDCD}	Shear, c.f Figure 4.5	$-\sqrt{2}/2$	$-\sqrt{2}/2$

Table 5.9: Material properties for paper in the interface model [5].

Notation	*Description*	*Inner*	*Outer*
K^0_{MD}	Initial stiffness in MD shear, c.f Figure 4.6	800 MPa	640 MPa
K^0_{ZD}	Initial stiffness in tension, c.f Figure 4.6	400 MPa	320 MPa
S^0_{MD}	Initial yield stress in MD shear, c.f Figure 4.6	1.45 MPa	1.18 MPa
S^0_{ZD}	Initial yield stress in tension, c.f Figure 4.6	0.45 Mpa	0.35 MPa
K^0_{CD}	Initial stiffness in CD shear, c.f Figure 4.6	800 MPa	640 Mpa
S_{CD}	Initial yield stress in CD shear, c.f Figure 4.6	1.45 Mpa	1.18 Mpa
A	Material constant, c.f Eq. 4.27	0.28	0.28
B	Material constant, c.f Eq. 4.27	0.8	0.8
C	Material constant, c.f Eq. 4.20	0.085	0.085
R^s_{ZD}	Residual strength factor in tension, c.f Eq. 4.21	0.97 Mpa	0.97 Mpa
R^s_{MD}	Residual strength factor in MD shear, c.f Eq. 4.21	0.87 Mpa	0.87 Mpa
R^s_{CD}	Residual strength factor in CD shear, c.f Eq. 4.21	0.87 MPa	0.87 MPa
R^k_{ZD}	Residual strength factor in tension, c.f Eq. 4.21	0.97 MPa	0.97 MPa
R^k_{MD}	Residual strength factor in MD shear, c.f Eq. 4.21	0.87 MPa	0.87 MPa
R^k_{CD}	Residual strength factor in CD shear, c.f Eq. 4.21	0.87 MPa	0.87 MPa

Table 5.10: Material properties for PET

	E [MPa]	ν [-]	*Stress [MPa]*	*Plastic strain [-]*
PET	3500	0.43	103	0
			220	1.05

5.6.2 Results of the 3DM simulations

In this section are the 3DM simulations verified with the experimental study, and in some cases compared with each other. In Figure 5.6 is one picture from the result in ABAQUS shown. It is obvious that it is possible for the paperboard to delaminate when the 3DM is employed. In Appendix B is the proceeding of the delamination and the amplitudes of the stresses shown.

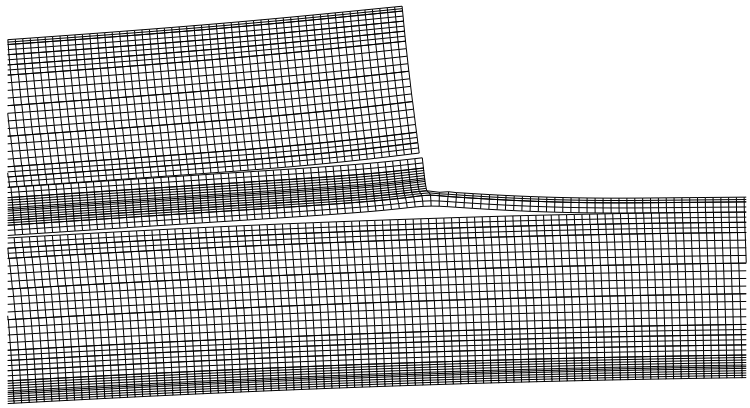

Figure 5.6: *The deformed shape of the model with 3DM employed*

In the presented curves in Figure 5.7 is the simulation of the overlap width 10 mm compared to the experimental curve with the overlap width 10.5 mm. The initial behavior and the hardening is captured very good by the simulation, but the ultimate strength is not predicted quite that well. The experiment gives an ultimate strength which is approximately 17% higher than the simulation, c.f Table 5.11.

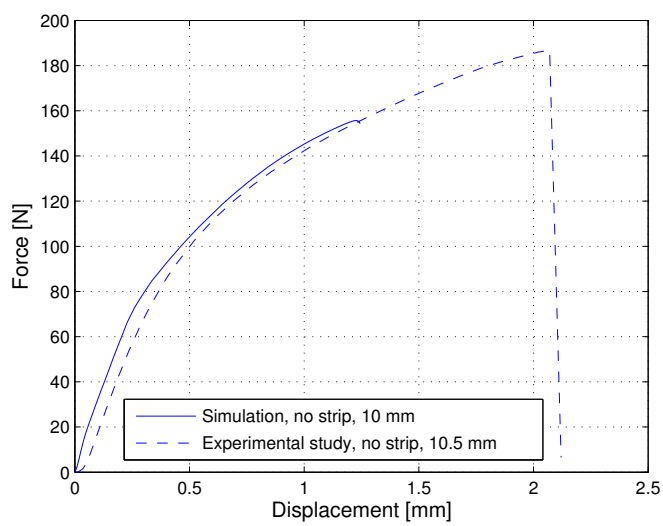

Figure 5.7: *Simulations compared to experimental data*

Since the model does not give a good prediction of the ultimate strength, the function $*$ STABILIZE in ABAQUS is used. This function applies springs that damps the model when local instabilities occur. A parameter is set to define the size of the damping and is by default $2e^{-4}$. In this case the damping is reduced and the parameter is set to $7e^{-6}$. Another function used in this simulation is $ANALYSIS = DISCONTINUOUS$, which allows a larger number of iterations before the convergence is checked. The functions are to be defined under the level *step* in the input file, see Appendix C. Unfortunately do these additional functions not improve the prediction very much as shown in Figure 5.8. The ultimate strength only increases marginally compared to the original simulation, but it is possible to follow the proceeding of the fracture propagation. Most likely are the input parameters in UMAT and UINTER somewhat wrong and therefore do the functions not improve the prediction.

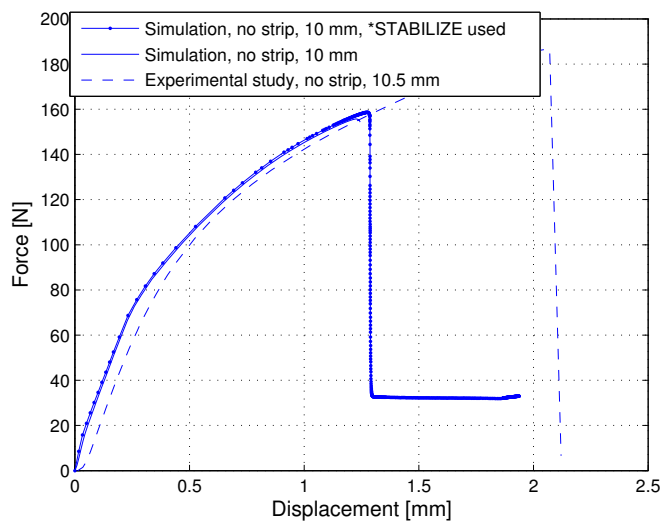

Figure 5.8: *Simulations with *STABILIZE compared to experimental data*

The *strip* and *folded strip* model show a similar initial behavior compared to the model *no strip* as shown in Figure 5.9. Though, the ultimate strengths in strip and folded strip are considerably higher, which partially is due to the strip that prevents delamination to some extent. The *folded strip* model shows quite another behavior when the 3DM is employed, c.f Figure 5.4. In the introductory models is the *folded strip* model considerably weaker than when the 3DM is employed.

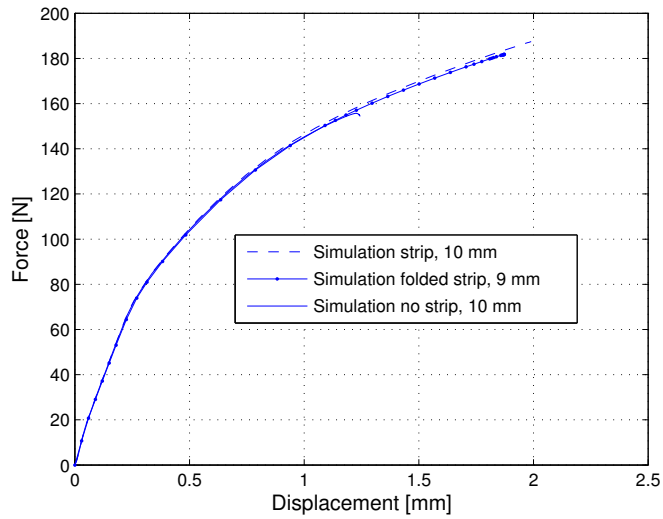

Figure 5.9: *Simulations of no strip, strip and folded strip*

In Figure 5.10 are the experimental results of the sealing type *folded strip* compared to the simulation. The simulation gives a good prediction, even for the ultimate strength which is slightly overestimated. One part of the reason to this is that the simulated overlap width is 9 mm whereas the tested overlap widths are 7.8 mm and 8.2 mm. In Table 5.11 are the ultimate strengths between the simulation and the experiment compared with each other. The simulation overestimates the experiment with approximately 5 %. The experimental value is in this table taken as a mean value from the experiment with an overlap width of 8.2 mm, since that is closest to the simulated overlap width of 9 mm.

Table 5.11: Comparison of simulation and experimental results.

Sealing type	*Ultimate strength experiment* [N]	*Ultimate strength simulation* [N]	*Difference* [%]
No strip	187.3*	155.7	16.9
Folded strip	173.9**	181.8	4.5

* *Mean value of all samples from test series 1 with the overlap width 10.5 mm*
** *Mean value of all samples with the overlap width 8.2 mm*

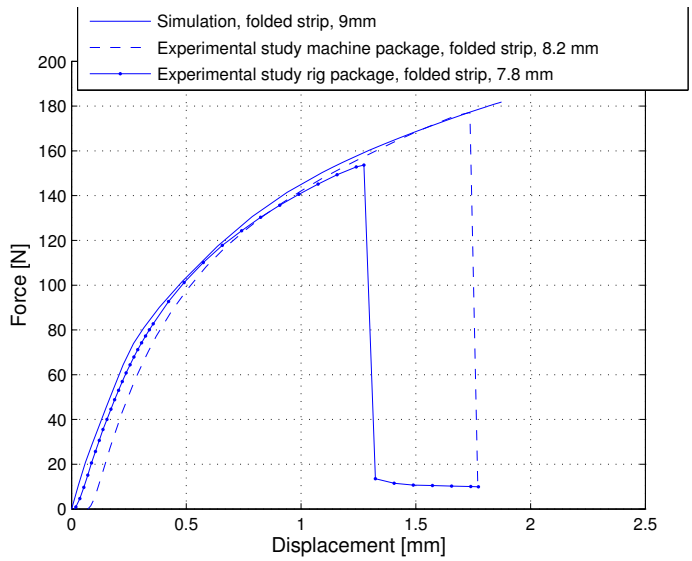

Figure 5.10: *Simulations and experimental results of folded strip*

The sealing type *edge to edge* was simulated with a $100\mu m$ thick PET strip on the inside and the outside and a strip width of 10 mm. It showed only a marginally stronger initial behavior than the sealing type *no strip*, which is shown in Figure 5.11. The ultimate strength on the other hand is significantly higher, even though it probably is not as high as in this simulation. Most likely, a fracture would occur in the paper and cause a failure before the ultimate strength is reached in this simulation. Compared to the *strip* simulation, as well as the *folded strip* simulation, the difference is not quite that remarkable as shown in Figure 5.12

In Figure 5.13 are the simulations for the case when MD is oriented in the horizontal length dimension also compared to the experimental results. For this case does the simulation not even capture the initial behavior. The simulation shows a much more stiff behavior the experimental data and the ultimate strength is not captured at all.

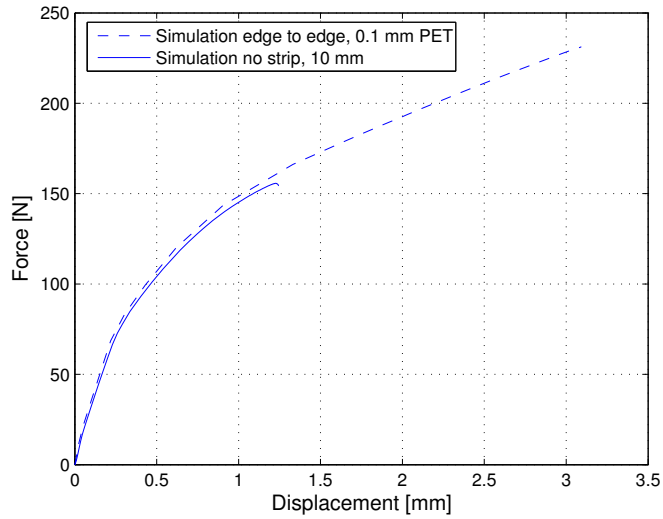

Figure 5.11: *Simulations of no strip and edge to edge*

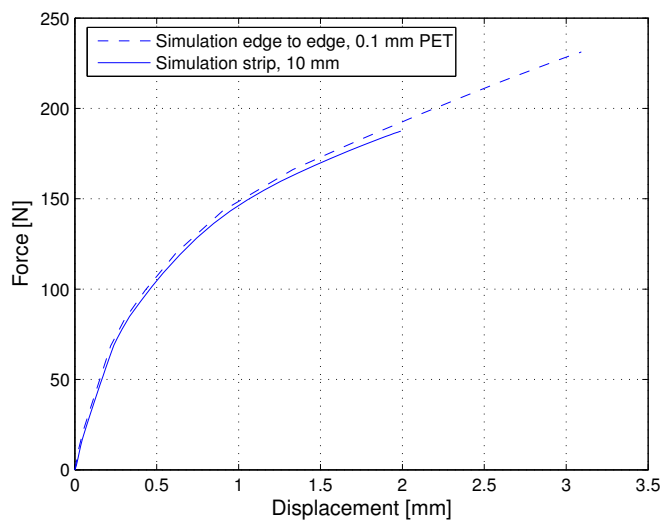

Figure 5.12: *Simulations of strip and edge to edge*

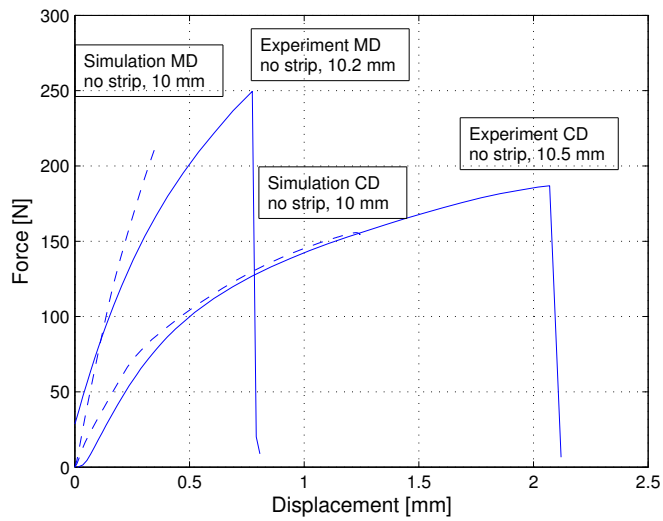

Figure 5.13: *Simulations and experimental results of no strip when MD and CD is oriented in the horizontal length dimension.*

Chapter 6

Numerical studies

6.1 General remarks

The numerical studies were accomplished in order to investigate which possible parameters that influence the mechanical behavior of the sealing in the simulations. In order to make it easier to draw conclusions from the simulations, the sealing type *no strip* was in all cases but one chosen for extensive studies. The parameters varied are shown in Table 6.1.

Table 6.1: The modified parameters.

Description	*Modified parameters*
Variation of the longitudinal overlap width	w
Variation of Young's modulus and the shear modulus of paper	E and G
Increased initial normal and shear stiffness for paper	$K^0_{MD}, K^0_{ZD}, K^0_{CD}$
Variation of the initial yield stress for paper	S^0_{zd}
Variation of thickness of the mechanical paper	t_{paper}
Decreased thickness of strip in the edge to edge model	t_{strip}

The longitudinal overlap width was varied from 5 to 25 mm with increments of 5 mm. As wide overlap widths as 25 mm are not likely to be manufactured, but in order to better predict the mechanical behavior of an overlap width variation, it was accomplished. In the variation of Young's modulus and the shear modulus of the paper, were the various modulus varied with $\pm 25\%$ from the original values used in Section 5.6.1. The initial normal and shear stiffness were increased with a factor 10. A factor 100 was also simulated, but that simulation was aborted early due to convergence problems. The initial yield stress was varied with $\pm 25\%$ compared to the original value in section 5.6.1. The thickness of the mechanical paper was set to $0.5t$ and $1.5t$ if the simulation in Chapter 5 is assumed to be t. The thickness of

the strip in the *edge to edge* model was decreased to $50\mu m$ from the original $100\mu m$ since a thickness of $100\mu m$ probably would be quite much.

6.2 Longitudinal overlap width variation

In this study, the influence of the mechanical behavior depending on the longitudinal overlap sealing width was studied. In Figure 6.1 are force-displacement curves for the various overlap widths $5, 10, 15, 20$ and 25 mm plotted. A wider overlap gives a stronger sealing, which is due to the smaller stresses that develops in ZD. When the overlap width is increased, the rotation of the cross section in Figure 2.4 is decreased and therefore are stresses in the ZD not developed in the same extension.

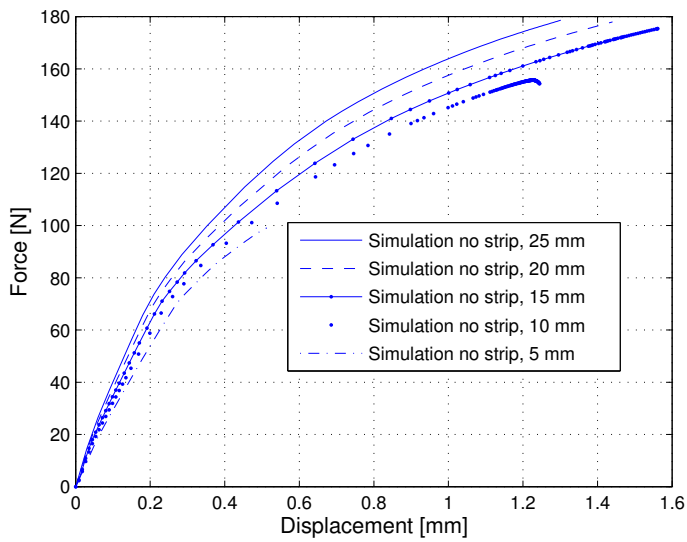

Figure 6.1: *Response curves of various overlap widths*

The ultimate strengths in the various simulations are somewhat different from the ultimate strengths in the experimental studies, as shown in Figure 6.2. The behavior is though fairly similar, but the ultimate strengths from the simulations are considerably lower.

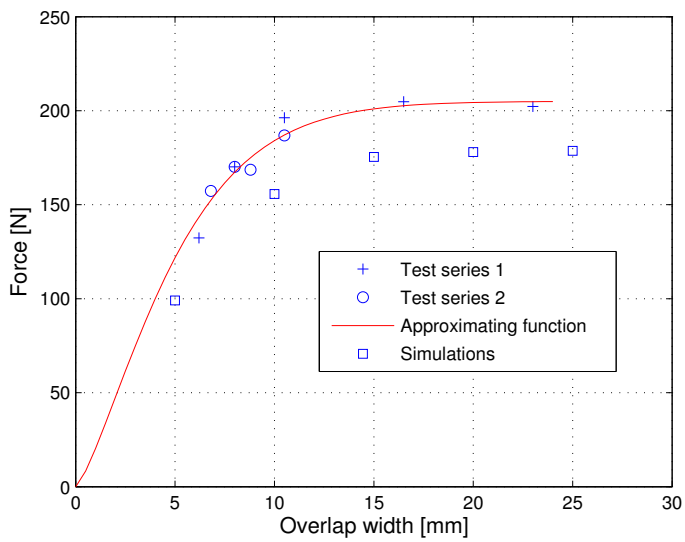

Figure 6.2: *Ultimate strength of experiment and simulations*

6.3 Young's modulus and shear modulus variation of paper

The purpose of this study was to investigate how the quality of the paper influences the mechanical behavior of the sealing. The modulus $E_{MD}, E_{ZD}, E_{CD}, G_{MDZD}, G_{MDCD}$ and G_{MDZD} were varied $\pm 25\%$ compared to the original material parameters. In Figure 6.3 is the relative variation in ultimate strength when Young's modulus E and the shear modulus G are modified, shown. The Young's modulus and the shear modulus seem to have a linear dependency on the ultimate strength of the sealing. A 25 % variation in these parameters gives only a slight variation in strength.

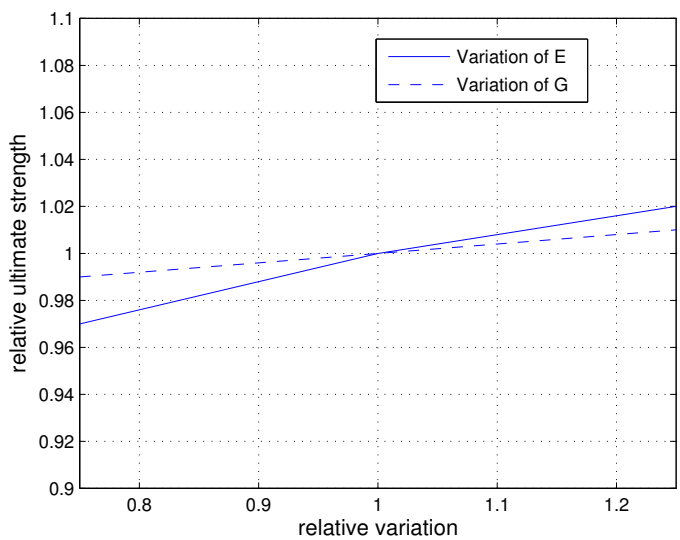

Figure 6.3: *Relative variation of Young's modulus and the shear modulus versus the relative ultimate strength.*

6.4 Increased initial stiffness parameters

In this study the initial stiffness parameters of the interface model were increased. This was made in order to get more accurate solutions since the original parameters were aimed to a model with less number of interfaces.

Increasing the initial stiffness parameters K^0_{MD}, K^0_{ZD} and K^0_{CD} ten times affects the simulation marginally, as shown in Figure 6.4. A simulation with hundred times the original parameters were also accomplished, but this simulation were aborted after only a few time frames due to convergence problems.

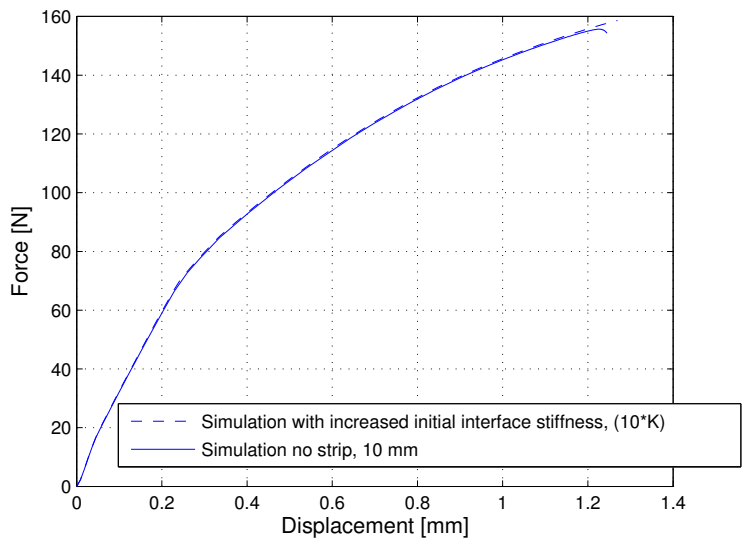

Figure 6.4: *Increase of the initial stiffness parameters in the interface model.*

6.5 Variation of the initial yield stress

The purpose of this study was to investigate how the initial yield stress in the thickness direction S_{zd}^0 influences the mechanical behavior of the sealing. It was varied with $\pm 25\%$ compared to the original value in Section 5.6.1. As shown in Figure 6.5 does the initial yield stress not affect the initial behavior and the hardening of the sealing. However, there is a difference in the ultimate strength as shown in Figure 6.5 and 6.6. The initial yield stress seems to have a nonlinear dependency on the ultimate strength, which can be explained by that a greater initial yield stress results in a slightly different final load case, which causes greater stresses in the ZD.

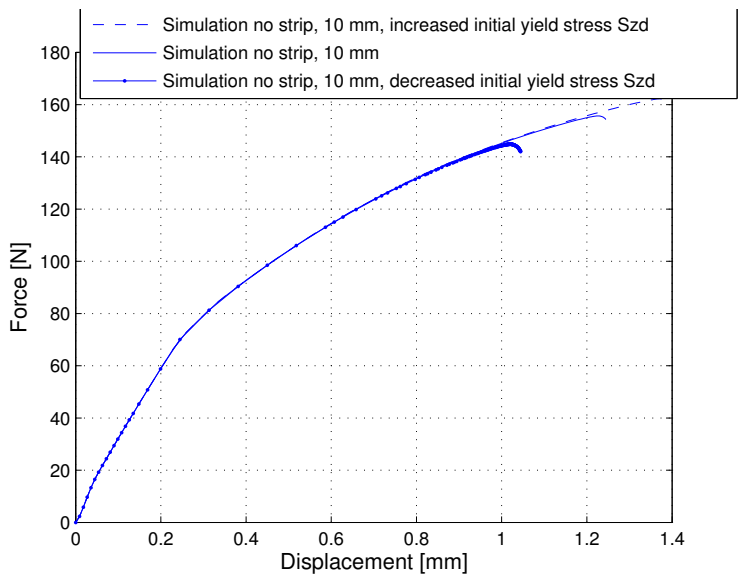

Figure 6.5: *Variation of the initial yield stress* S_{zd}

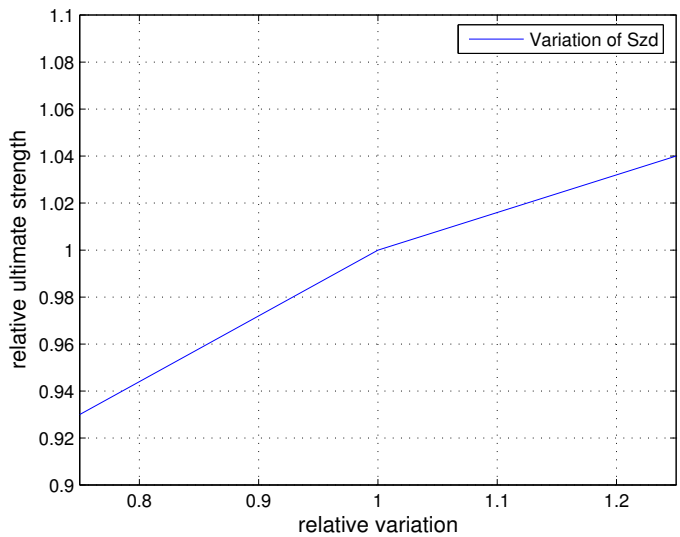

Figure 6.6: *Relative variation of the initial yield stress S_{zd} versus the relative ultimate strength.*

6.6 Thickness variation of paper

In this study, the influence of the thickness of the mechanical paper on the mechanical behavior of the sealing was investigated. Changing the thickness of the mechanical paper seems to affect the behavior of the sealing remarkably. The initial behavior and the hardening of the sealing changes as could be expected, see Figure 6.7. A thinner paperboard gives a less stiff response, whereas the simulation with the thicker paper reaches the plastic region later. The significant result in this study is the ultimate strength which not seems to be depending on the thickness of the mechanical paper. Less paper gives as high ultimate strength as those simulations with thicker paper do, but it is reached at larger strains. When the ultimate strength is reached at larger strains, it requires more mechanical work to cause failure in the specimen, since the area below the curve gives the mechanical work. Though it must be noted that when the thickness is decreased, the initial interface stiffness parameters ought to be increased to get an accurate response of the sealing. Since the increased initial stiffness parameters in Section 6.4 only gives a modest change in behavior of the sealing, this was not accomplished.

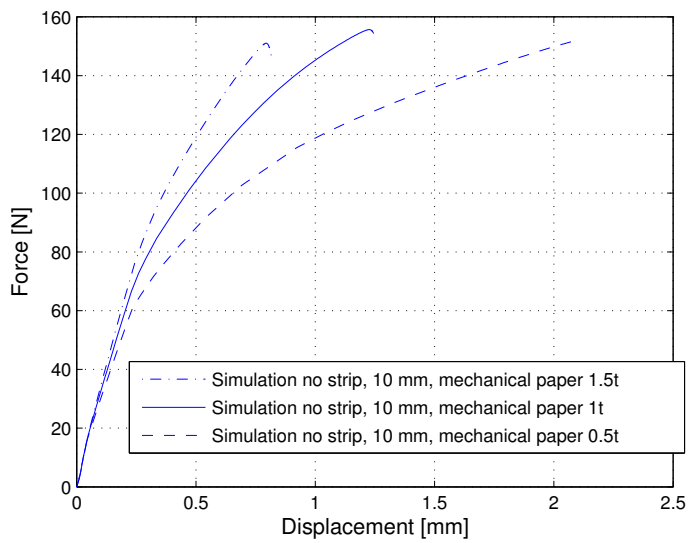

Figure 6.7: *Variation of thickness of the mechanical paper*

6.7 Decreased thickness of strip

In this study it was investigated how a thinner strip in the *edge to edge* model influences the mechanical behavior of the sealing. Since a thickness of each strip of $100\mu m$ for the two strips is rather large, it was decreased to $50\mu m$. The behavior of the two simulations were similar, but failure occurred earlier when the thickness was decreased, as shown in Figure 6.8. All the loading has to be transferred by the strips into the laminate, thus a thinner strip results in a slightly weaker behavior.

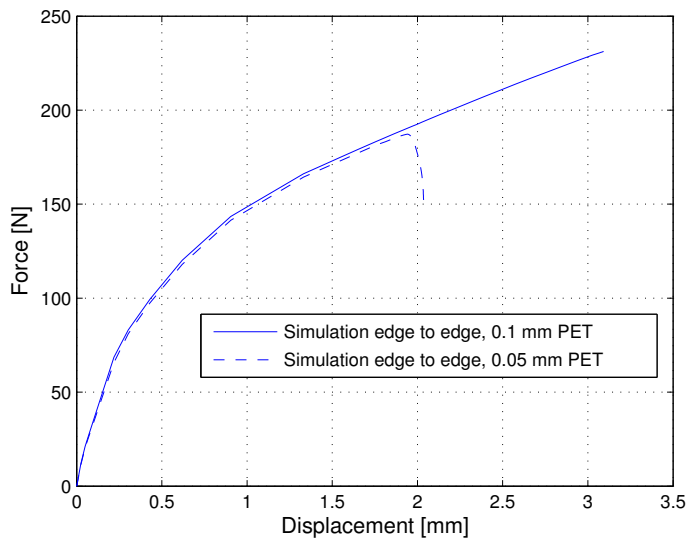

Figure 6.8: *Variation of thickness of the PET-strip*

Chapter 7

Discussion

The tension tests performed of the LS shows an initial elastic part followed by plastic behavior and kinematic hardening. The mechanical behavior of the LS is determined by the properties of the laminate, whereas the ultimate strength of the sealing is determined by the geometry and the of the sealing and the material properties of the paper.

The longitudinal overlap width has significant influence on the the mechanical behavior of the sealing up to a width of approximately 12 mm, due to the decreasing rotation of the cross section. From the experimental tests it was concluded that an increase of the overlap width from 8.0 to 10.5 mm (31.3 %) increases the ultimate strength from 170.2 N to 196.2 N (15.2 %). The mechanical work required increases at the same time from 189.1 Nmm to 282.1 Nmm (49 %), which is quite remarkable.

The FE-simulations with the 3DM employed shows very good agreement with the experimental tests for the case when the CD is oriented in the horizontal length dimension. The ultimate strength is difficult to capture, especially for the sealing type *no strip*, but the overall mechanical behavior is very well predicted.

The *edge to edge* sealing remarkably reduces the stresses in the ZD, since there is no rotation of the cross section as in the overlap sealings. Therefore it manages to be subjected to higher loads. The *strip* and *folded strip* sealing have very similar behavior. The most interesting difference is that the *strip* sealing may to be subjected to some loading after the fracture has propagated through the paperboard, which the *folded strip* cannot do. Therefore is the mechanical work required to break the *strip* sealing somewhat higher compared to the *folded strip* sealing.

The paper thickness seem to have great influence of the mechanical behavior of the sealing. A decrease of the paper thickness does not influence the ultimate strength, but it gives a more ductile fracture with a higher mechanical work required, see Figure 6.7. Unfortunately is the paper thickness also a parameter with great influence on the grip stiffness of a package, see Andreasson and Bengtsson [3].

7.1 Proposals for future work

From the results in this work it has been shown that the 3DM shows quite good agreement with reality for tension load cases in CD. The future work could therefore focus on the following subjects:

- Why there is worse agreement for the MD case
- Try to capture the ultimate strength in the simulations in a better way.
- The relationship between the height of fall for a package and the mechanical influence of the longitudinal sealing or
- A model of an entire package simulating a fall
- A more thorough investigation of the sealing type *edge to edge*, for example an experimental study.
- Determine whether it is a high ultimate strength or a high mechanical work required to break the sealing that is most important to receive a sealing with good performance.

Bibliography

[1] ABAQUS Inc., (2005) *ABAQUS/Standard manuals, version 6.5*, Pawtucket, RI, USA.

[2] Andersson H., (1998) *IH sealing: Induction Heating as sealing method at Tetra Pak*,Tetra Pak Research & Developement AB, Sealing Technology, Lund

[3] Andreasson E. and Bengtsson T., (2002) *Grip stiffness in beverage packages - An experimental and finite element study*,Division of Structural Mechanics, Lund University, Sweden.

[4] Elison O. and Hansson L., (2005) *Evaluating the 3DM model - an experimental and finite element study*, Division of Solid Mechanics, Lund University, Sweden.

[5] Nygårds M.,(2005), *The 3DM model 3.22*, STFI-Packforsk

[6] Ottosen N.S. and Petersson H.,(1992), *Introduction to the Finite Element Method*, Prentice Hall Europe, Great Britain.

[7] Ottosen N.S. and Ristinmaa M.,(1999), *The Mechanics of Constitutive Modelling, Volume 1, Classical topics*, Division of Solid Mechanics, Lund University, Sweden.

[8] Persson K., (1991), *Material model for paper: Experimental and Theoretical Aspects*, Divison of Structural Mechanics, Lund University, Sweden.

[9] Xia Q.S., (2002), *Mechanics of inelastic deformation and delamination in paperboard*, Department of Mechanical Engineering, Massachusetts Institute of Technology, Cambridge, MA, USA

[10] www.tetrapak.com. 20050908

Appendix A

Results from experimental tests

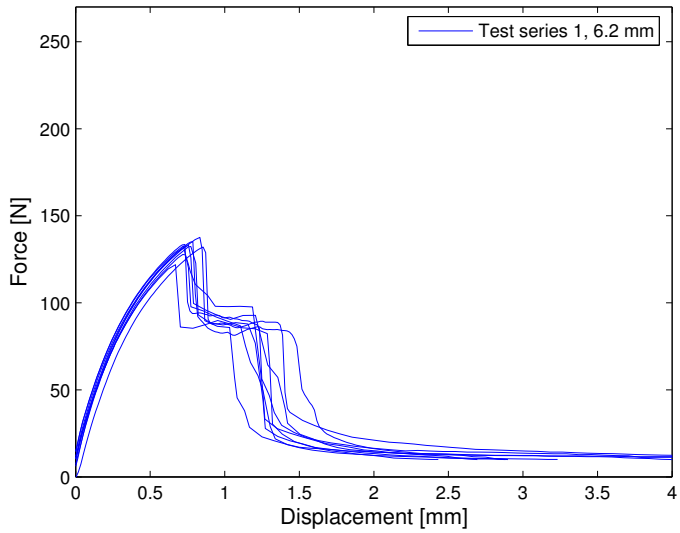
Test series 1, 6.2 mm
Force [N]
Displacement [mm]
0
50
100
150
200
250
0
0.5
1
1.5
2
2.5
3
3.5
4

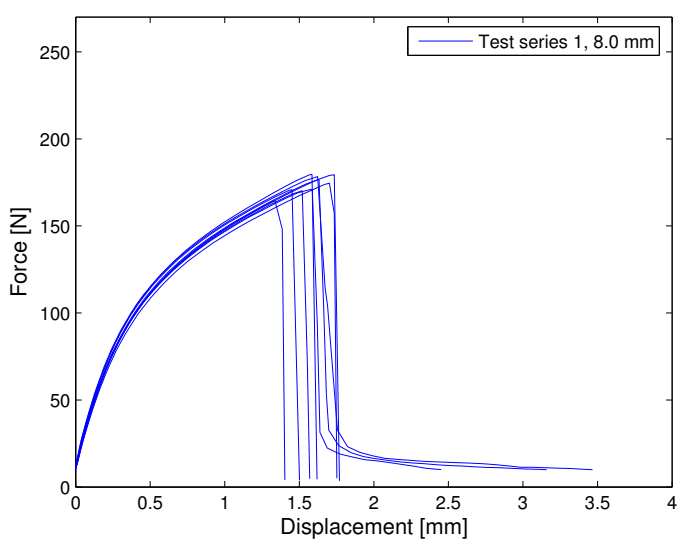
Test series 1, 8.0 mm
Force [N]
Displacement [mm]
0
50
100
150
200
250
0
0.5
1
1.5
2
2.5
3
3.5
4

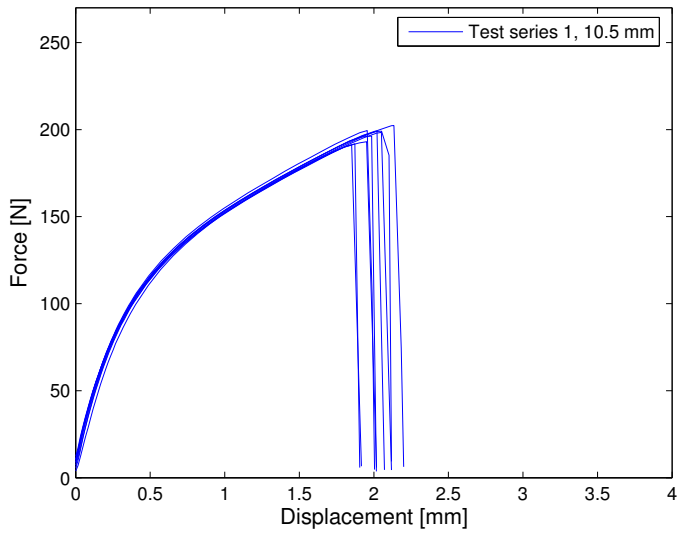
Test series 1, 10.5 mm
Force [N]
Displacement [mm]
0
50
100
150
200
250
0
0.5
1
1.5
2
2.5
3
3.5
4

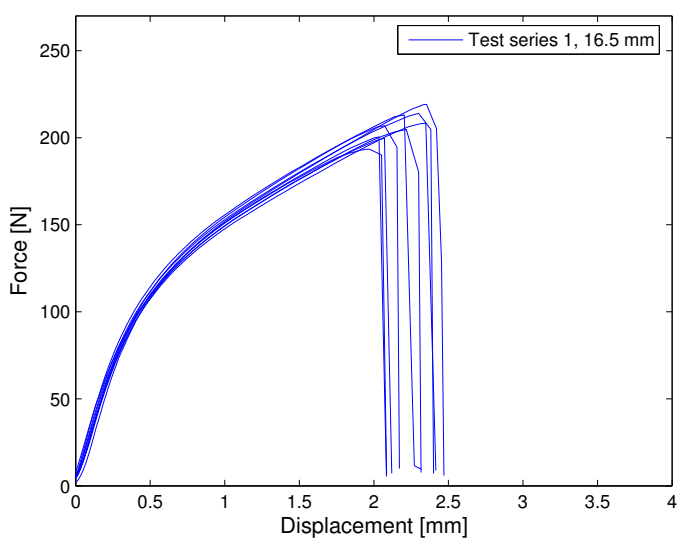
Test series 1, 16.5 mm
Force [N]
Displacement [mm]
0
50
100
150
200
250
0
0.5
1
1.5
2
2.5
3
3.5
4

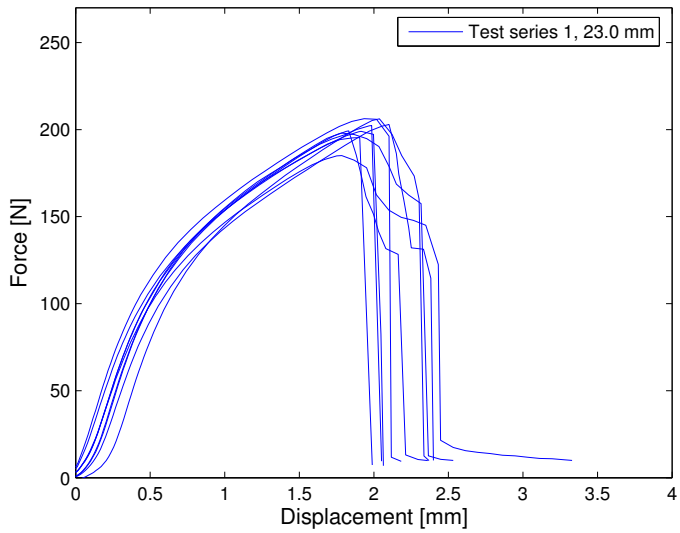
Test series 1, 23.0 mm
Force [N]
Displacement [mm]
0
50
100
150
200
250
0
0.5
1
1.5
2
2.5
3
3.5
4

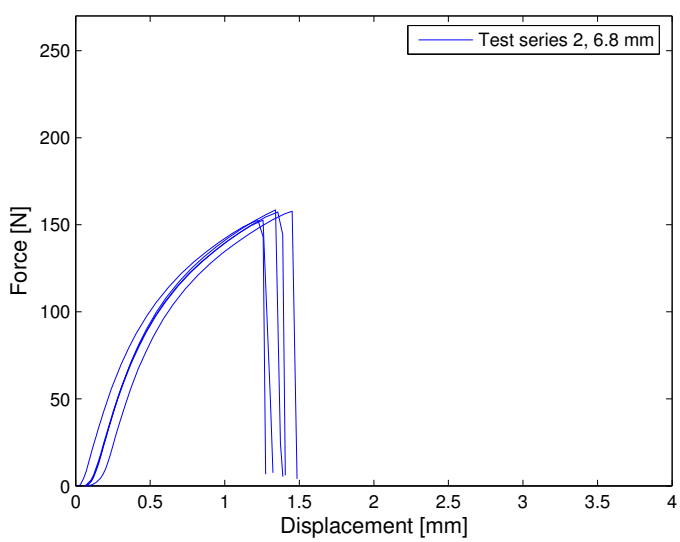
Test series 2, 6.8 mm
Force [N]
Displacement [mm]
0
50
100
150
200
250
0
0.5
1
1.5
2
2.5
3
3.5
4

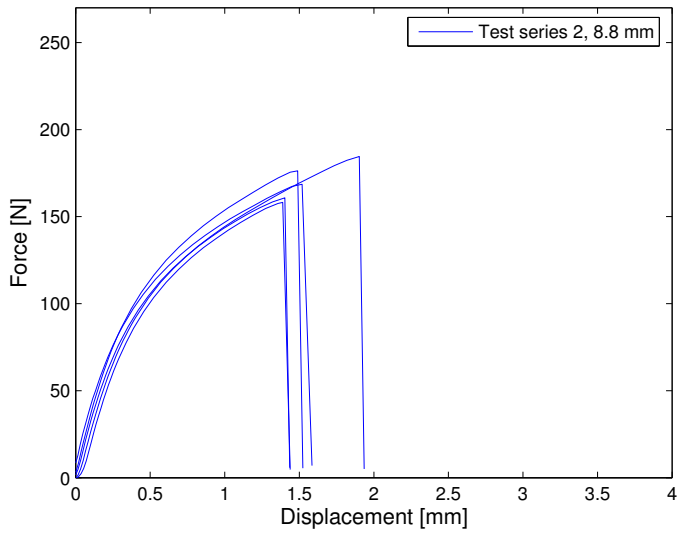
Test series 2, 8.8 mm
Force [N]
Displacement [mm]
0
50
100
150
200
250
0
0.5
1
1.5
2
2.5
3
3.5
4

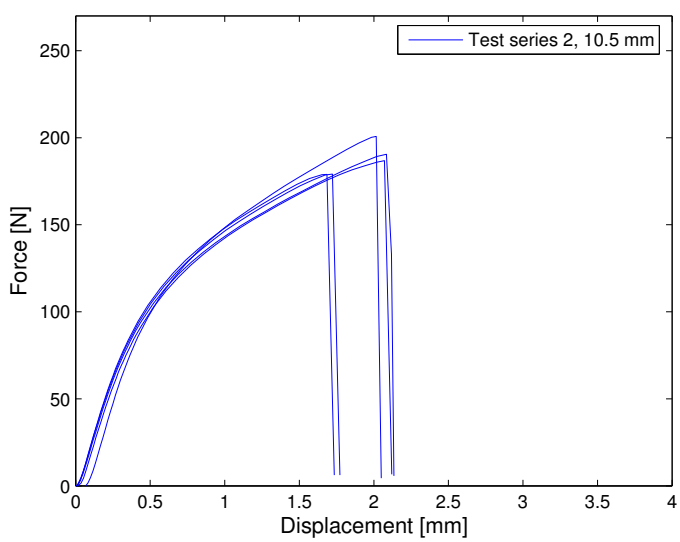
Test series 2, 10.5 mm
Force [N]
Displacement [mm]
0
50
100
150
200
250
0
0.5
1
1.5
2
2.5
3
3.5
4

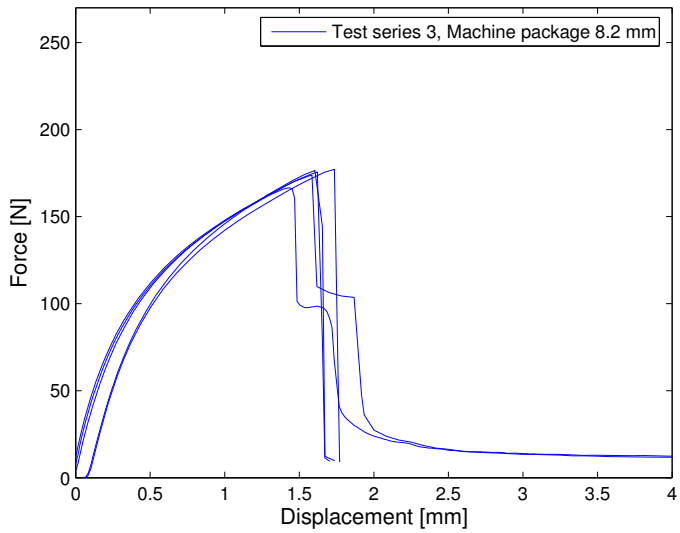
Test series 3, Machine package 8.2 mm
Force [N]
Displacement [mm]
0
50
100
150
200
250
0
0.5
1
1.5
2
2.5
3
3.5
4

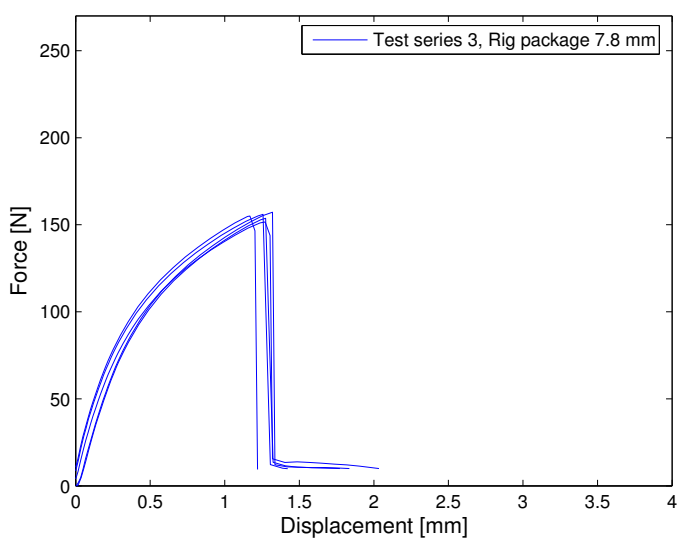
Test series 3, Rig package 7.8 mm
Force [N]
Displacement [mm]
0
50
100
150
200
250
0
0.5
1
1.5
2
2.5
3
3.5
4

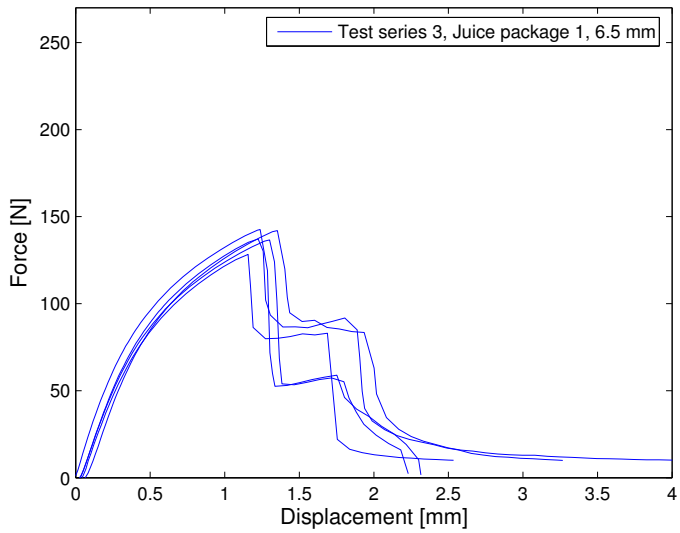
Test series 3, Juice package 1, 6.5 mm
Force [N]
Displacement [mm]
0
50
100
150
200
250
0
0.5
1
1.5
2
2.5
3
3.5
4

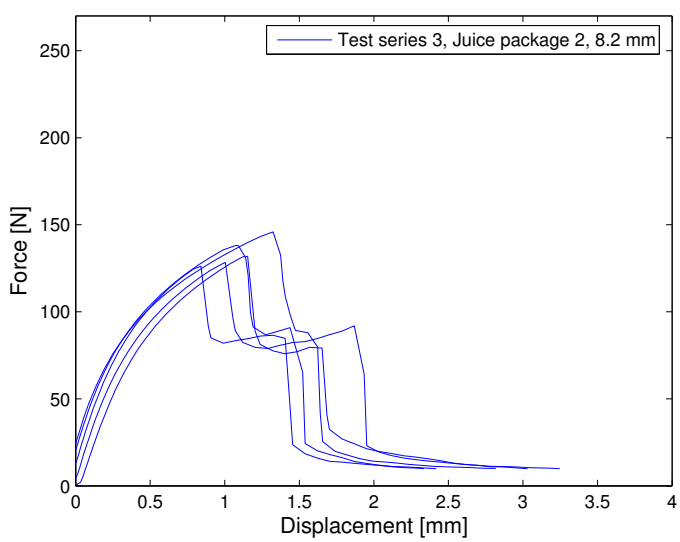
Test series 3, Juice package 2, 8.2 mm
Force [N]
Displacement [mm]
0
50
100
150
200
250
0
0.5
1
1.5
2
2.5
3
3.5
4

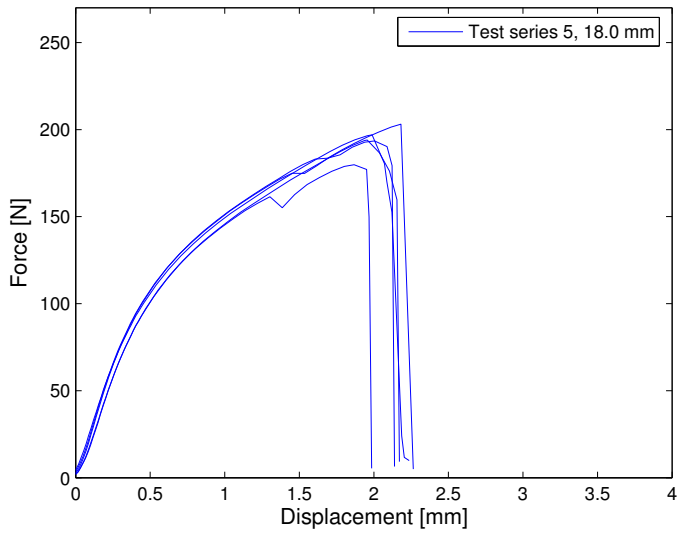
Test series 5, 18.0 mm
Force [N]
Displacement [mm]
0
50
100
150
200
250
0
0.5
1
1.5
2
2.5
3
3.5
4

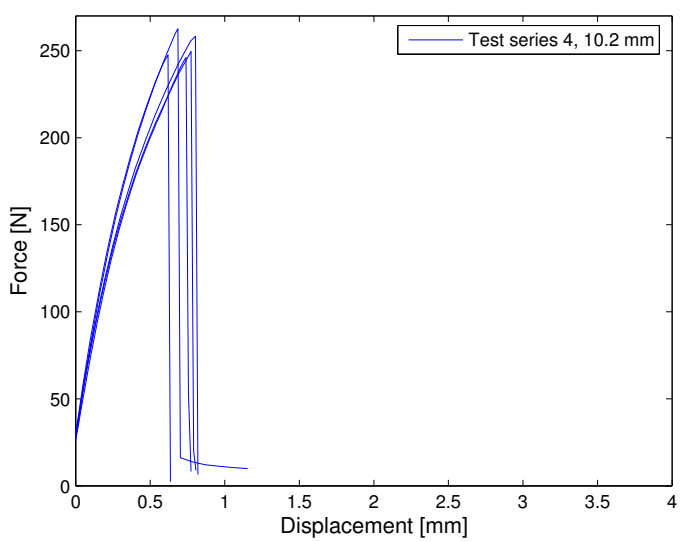
Test series 4, 10.2 mm
Force [N]
Displacement [mm]
0
50
100
150
200
250
0
0.5
1
1.5
2
2.5
3
3.5
4

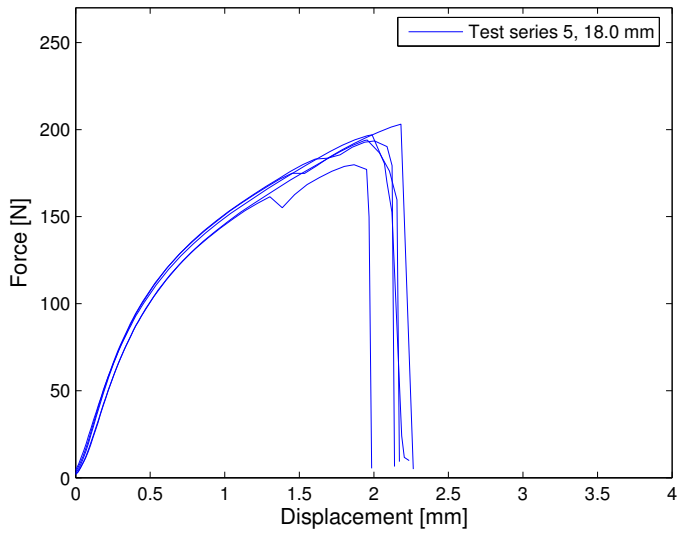
Test series 5, 18.0 mm
Force [N]
Displacement [mm]
0
50
100
150
200
250
0
0.5
1
1.5
2
2.5
3
3.5
4

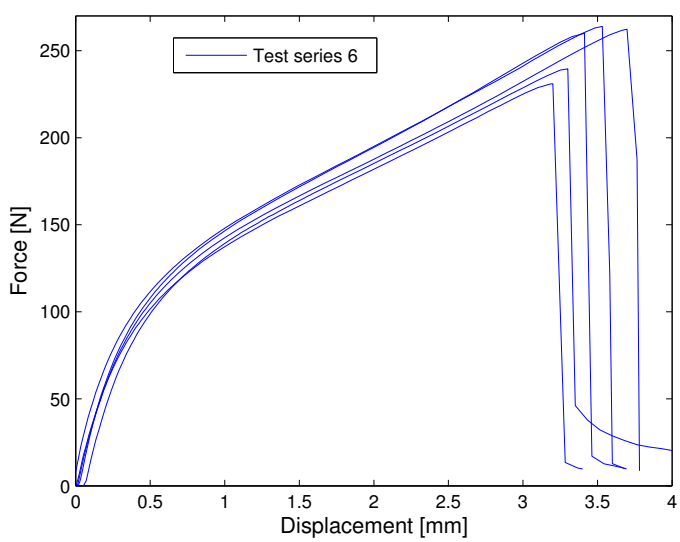
Test series 6
Force [N]
Displacement [mm]
0
50
100
150
200
250
0
0.5
1
1.5
2
2.5
3
3.5
4

Appendix B

Results from simulation

Figure B.1: S_{11}, *time frame 0*

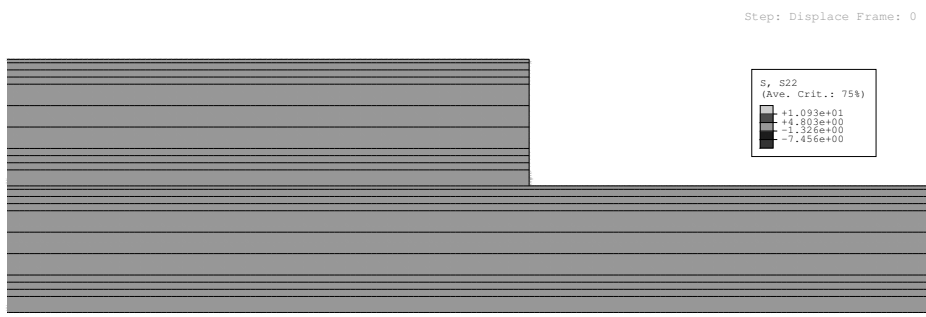

Figure B.2: S_{22}, *time frame 0*

Figure B.3: S_{12}, *time frame 0*

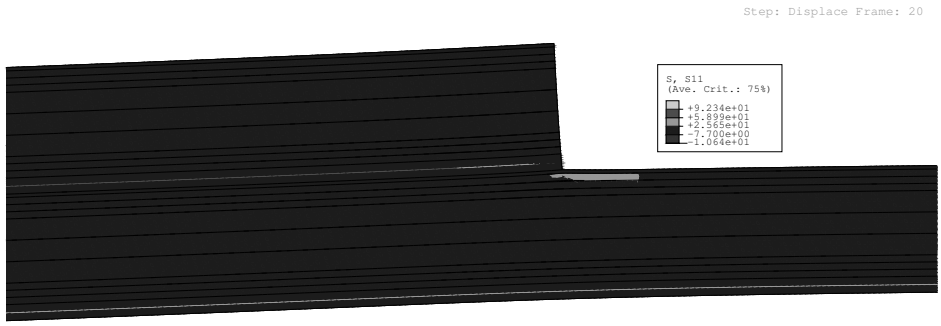

Figure B.4: S_{11}, *time frame 20*

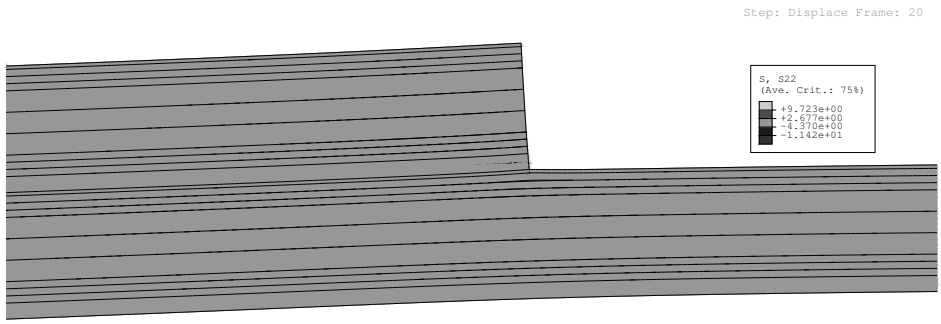

Figure B.5: S_{22}, *time frame 20*

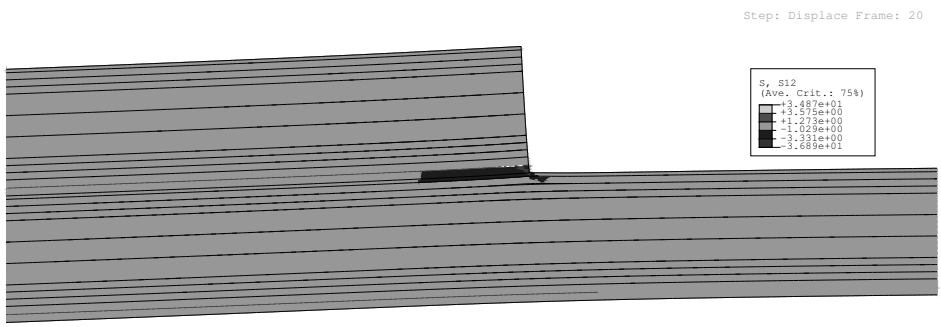

Figure B.6: S_{12}, *time frame 20*

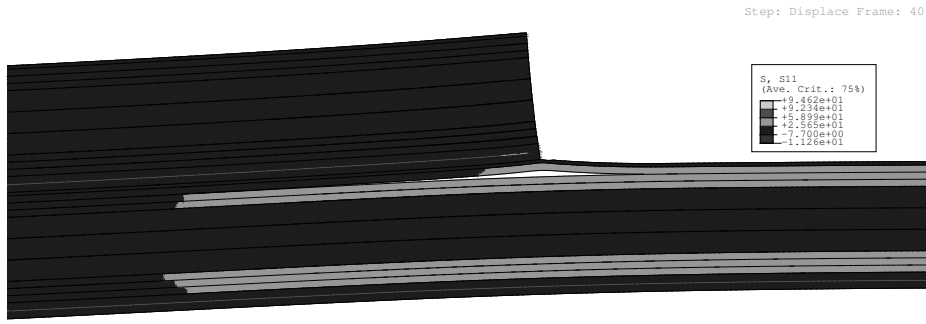

Figure B.7: S_{11}, *time frame 40*

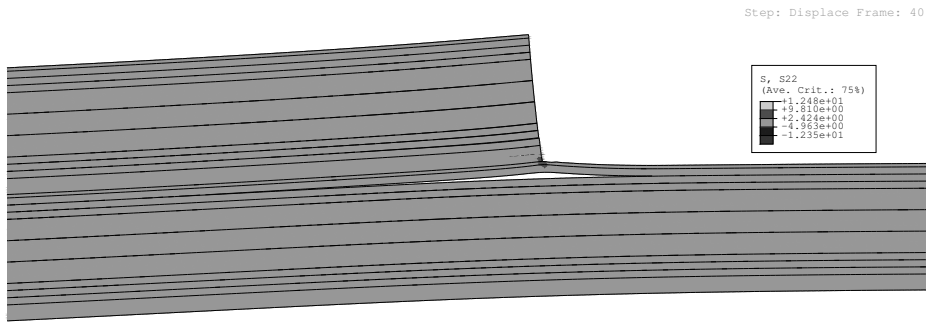

Figure B.8: S_{22}, *time frame 40*

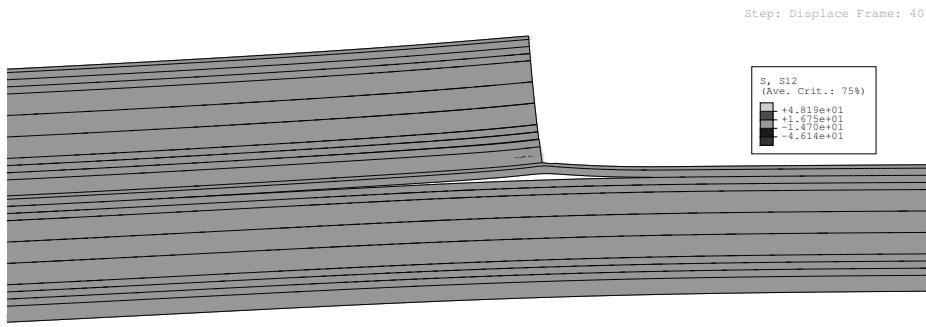

Figure B.9: S_{12}, *time frame 40*

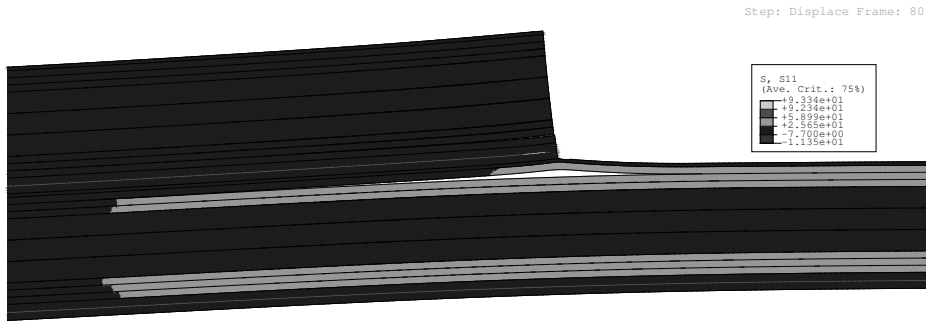

Figure B.10: S_{11}, *time frame 80*

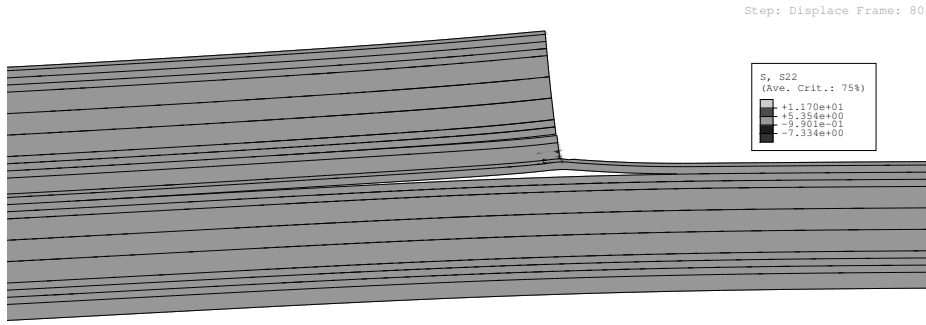

Figure B.11: S_{22}, *time frame 80*

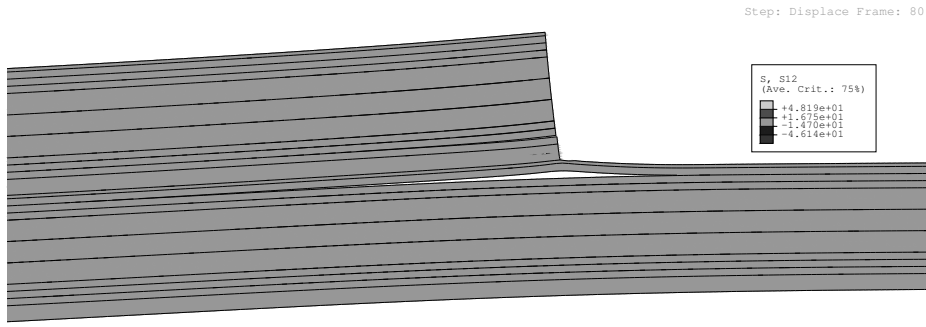

Figure B.12: S_{12}, *time frame 80*

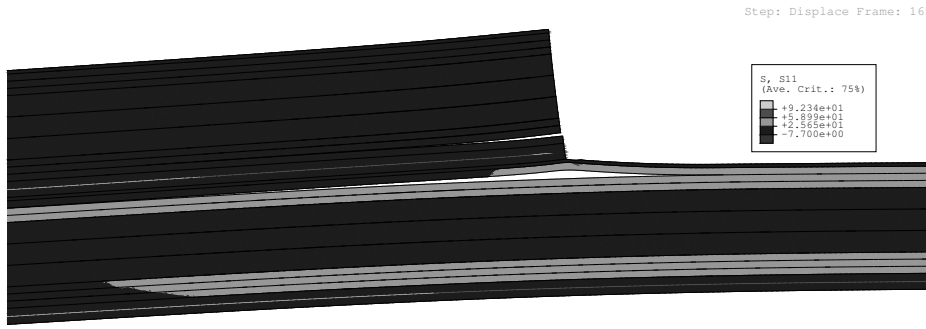

Figure B.13: S_{11}, *time frame 165*

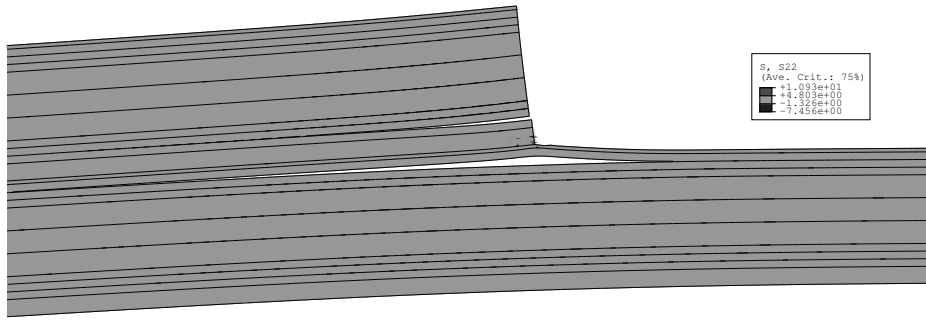

Figure B.14: S_{22}, *time frame 165*

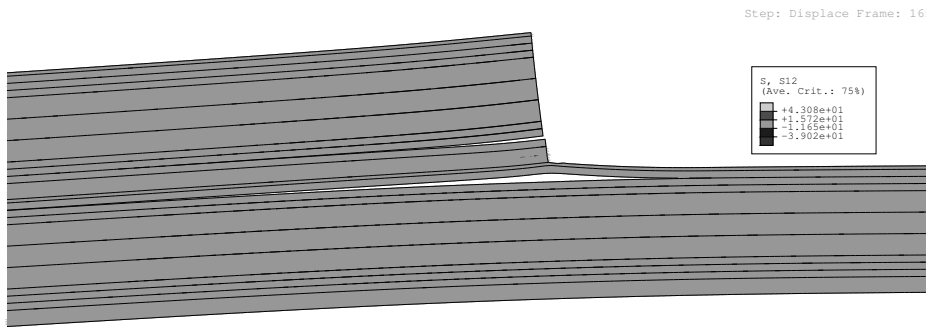

Figure B.15: S_{12}, *time frame 165*

Appendix C

ABAQUS Input File

An example of an input file for ABAQUS. The sealing type was *no strip* and the longitudinal overlap width was set to 10 mm.

```
*Heading ** Job name: 3dm_10 Model name: NoStrip_3dm_10 *Preprint,
echo=NO, model=NO, history=NO, contact=NO **
**-----------------------------------------------------------------------------------------
** **                  PARTS **
**-----------------------------------------------------------------------------------------
*Part, name=LDPE_AL_LK_Low *Node
      1,           3.,   2.06100011
      2,           3.,   2.03399992
      3,          18.,   2.03399992
       .
       .
       .
  10901,  -11.9799995,      2.05425
**
*Element, type=CPE4
  1,    1,   13, 3986,  496
  2,   13,   14, 3987, 3986
  3,   14,   15, 3988, 3987
   .
   .
   .
9900, 10901,  3982,    12,  3983
**
*Solid Section, elset=Set-MTRL_LDPE_Bot, material=LDPE
15.,
**
*Solid Section, elset=Set-MTRL_ALU, material=Alu
15.,
**
*Solid Section, elset=Set-MTRL_LK, material=LK
15.,
**
*End Part
**
*Part, name=LDPE_AL_LK_Up
*Node
      1,           3.,   2.06100011
      2,           3.,   2.03399992
      3,          18.,   2.03399992
       .
       .
       .
  10899,     -11.9375,   2.04075003
  10900,     -11.9375,    2.0474999
  10901,     -11.9375,      2.05425
**
*Element, type=CPE4
   1,    1,   13, 3986, 1516
   2,   13,   14, 3987, 3986
   3,   14,   15, 3988, 3987
    .
    .
    .
9900, 10901,  3982,    12,  3983
**
**
*Solid Section, elset=Set-MTRL_LDPE_Bot, material=LDPE
15.,
**
*Solid Section, elset=Set-MTRL_ALU, material=Alu
15.,
**
*Solid Section, elset=Set-MTRL_LK, material=LK
15.,
**
*End Part
**
```

```
**----------------------------------------
*Part, name=LDPE_Top
*Node
      1,           6.,           1.
      2,           6.,   1.01300001
      3,          -9.,   1.01300001
       .
       .
       .
   2973,   20.9799995,   1.00650001
**
*Element, type=CPE4
  1,    1,    7, 1986,  486
  2,    7,    2,    8, 1986
  3,  486, 1986, 1987,  485
   .
   .
   .
1980, 2973, 1235,    5, 1236
**
*Solid Section, elset=Set-MTRL_LDPE_Top, material=LDPE
15.,
**
*End Part
**
**----------------------------------------
*Part, name=PAPER_IN
*Node
      1,           5.,           3.
      2,           5.,   3.08159995
      3,         -10.,   3.08159995
       .
       .
       .
   4955,   19.9799995,   3.02040005
**
*Element, type=CPE4
  1,    1,    7, 1992,  490
  2,    7,    8, 1993, 1992
  3,    8,    9, 1994, 1993
   .
   .
   .
3960, 4955, 1239,    5, 1240
**
*Solid Section, elset=Set-MTRL_PAPER_IN, material=Paper_Mech
15.,
**
*End Part
**
**----------------------------------------
*Part, name=PAPER_OUT
*Node
      1,           6.,           2.
      2,           6.,   2.02719998
      3,          -9.,   2.02719998
       .
       .
       .
   2973,   20.9799995,   2.01360011
**
*Element, type=CPE4
  1,    1,    7, 1986,  486
  2,    7,    2,    8, 1986
  3,  486, 1986, 1987,  485
   .
   .
```

```
   .
1980, 2973, 1235,    5, 1236
**
*Solid Section, elset=Set-MTRL_PAPER_OUT, material=Paper_Chem
15.,
**
*End Part
**
**----------------------------------------------------------------------------------------
**
**                  CONSTRAINTS
**
**----------------------------------------------------------------------------------------
**
** Constraint: NoSlip_Betw_Layer
*Tie, name=NoSlip_Betw_Layer, adjust=yes
Surf_Low_Up:U, Surf_Low_Up:O
**
** Constraint: NoSlip_LDPE_Top-Paper_Low
*Tie, name=NoSlip_LDPE_Top-Paper_Low, adjust=yes
Surf_Low:LDPE-TopPly_U, Surf_Low:LDPE-TopPly_O
**
** Constraint: NoSlip_LDPE_Top-Paper_Up
*Tie, name=NoSlip_LDPE_Top-Paper_Up, adjust=yes
Surf_Up:LDPE-TopPLy_U, Surf_Up:LDPE-TopPLy_O
**
** Constraint: NoSlip_Paper-LDPE_Bot_Low
*Tie, name=NoSlip_Paper-LDPE_Bot_Low, adjust=yes
Surf_Low:BotPly_Bot-LDPE_Bot_U, Surf_Low:BotPly_Bot-LDPE_Bot_O
**
** Constraint: NoSlip_Paper-LDPE_Bot_Up
*Tie, name=NoSlip_Paper-LDPE_Bot_Up, adjust=yes
Surf_Up:BotPly_Bot-LDPE_Bot_U, Surf_Up:BotPly_Bot-LDPE_Bot_O
**
** Constraint: Reference
*Coupling, constraint name=Reference, ref node=RF, surface=Disp
*Kinematic
*End Assembly
**----------------------------------------------------------------------------------------
**
**                  MATERIALS
**
**----------------------------------------------------------------------------------------
**
*Material, name=Alu
*Elastic
70000., 0.3
**
*Plastic
50.,     0.
80., 0.0193
**
**
*Material, name=LDPE
*Elastic
150., 0.35
**
*Plastic
 9.,    0.
10., 0.002
11.,    1.
**
**
*Material, name=LK
*Elastic
300., 0.35
**
```

```
*Plastic
18.,    0.
20., 0.002
22.,    1.
**
**
*Material, name=Paper_Chem
*Depvar
     45,
*User Material, constants=44, unsymm
     3400.,     25.,   8900.,      0.,    0.14,      0.,     38.,   2400.
     58.,      0.,     5.4,     1.5,     1.5,      4.,     16.5,    22.
      8.,     6.3,     6.3,     7.4,     44.,     18.,     12.5,    12.
    160.,    260.,    375.,    310.,    160.,    160.,    800.,    200.
    225.,    300.,  0.9912, -0.1322, -0.4472,  0.8944,  0.7071, -0.9912
  0.1322,  0.4472, -0.8944, -0.7071
**
**
*Material, name=Paper_Mech
*Depvar
     45,
*User Material, constants=44, unsymm
     960.,     16.,    3400.,      0.,    0.10,      0.,     15.,    800.
     20.,      0.,     5.4,     1.5,     1.5,      4.,    6.5,     10.7
      6.,     6.3,     6.3,     7.4,     19.,     7.5,      9.,      6.
    160.,    260.,    375.,    310.,    160.,    160.,    800.,    200.
    225.,    300.,  0.9912, -0.1322, -0.4472,  0.8944,  0.7071, -0.9912
  0.1322,  0.4472, -0.8944, -0.7071
**
**----------------------------------------------------------------------------------------
**
**              INTERACTION PROPERTIES
**
**----------------------------------------------------------------------------------------
**
*Surface Interaction, name=IntProp_Mid-Mid, USER, DEPVAR=20, PROPERTIES=15, UNSYMM
 15
 640.0, 320.0, 1.18, 0.35, 640.0, 1.18, 0.28, 0.8,
 0.085,  0.97, 0.87, 0.87,  0.97, 0.87, 0.87
**
**
*Surface Interaction, name=IntProp_Mid-Out, USER, DEPVAR=20, PROPERTIES=15, UNSYMM
 15
 800.0, 400.0, 1.45, 0.45, 800.0, 1.45, 0.28, 0.8,
 0.085,  0.97, 0.87, 0.87,  0.97, 0.87, 0.87
**
**
*Surface Interaction, name=IntProp_Out-Out, USER, DEPVAR=20, PROPERTIES=15, UNSYMM
 15
 800.0, 400.0, 1.45, 0.45, 800.0, 1.45, 0.28, 0.8,
 0.085,  0.97, 0.87, 0.87,  0.97, 0.87, 0.87
**
**----------------------------------------------------------------------------------------
**
**              INTERACTIONS
**
**----------------------------------------------------------------------------------------
**
** Interaction: Inter_BotPly_1_Low
*Contact Pair, interaction=IntProp_Out-Out
Surf_Low:BotPly_Top-Mid_U, Surf_Low:BotPly_Top-Mid_O
**
**
** Interaction: Inter_BotPly_1_Up
*Contact Pair, interaction=IntProp_Out-Out
Surf_Up:BotPly_Top-Mid_U, Surf_Up:BotPly_Top-Mid_O
**
```

```
**
** Interaction: Inter_BotPly_2_Low
*Contact Pair, interaction=IntProp_Out-Out
Surf_Low:BotPly_Mid-Bot_U, Surf_Low:BotPly_Mid-Bot_O
**
**
** Interaction: Inter_BotPly_2_Up
*Contact Pair, interaction=IntProp_Out-Out
Surf_Up:BotPly_Mid-Bot_U, Surf_Up:BotPly_Mid-Bot_O
**
**
** Interaction: Inter_MidPly-BotPly_Low
*Contact Pair, interaction=IntProp_Mid-Out
Surf_Low:MidPly_Bot-BotPly_Top_U, Surf_Low:MidPly_Bot-BotPly_Top_O
**
**
** Interaction: Inter_MidPly-BotPly_Up
*Contact Pair, interaction=IntProp_Mid-Out
Surf_Up:MidPly_Bot-BotPLy_Top_U, Surf_Up:MidPly_Bot-BotPly_Top_O
**
**
** Interaction: Inter_MidPly_1_Low
*Contact Pair, interaction=IntProp_Mid-Mid
Surf_Low:MidPly_Top-Mid_U, Surf_Low:MidPly_Top-Mid_O
**
**
** Interaction: Inter_MidPly_1_Up
*Contact Pair, interaction=IntProp_Mid-Mid
Surf_Up:MidPly_Top-Mid_U, Surf_Up:MidPly_Top-Mid_O
**
**
** Interaction: Inter_MidPly_2_Low
*Contact Pair, interaction=IntProp_Mid-Mid
Surf_Low:MidPly_Mid-Bot_U, Surf_Low:MidPly_Mid-Bot_O
**
**
** Interaction: Inter_MidPly_2_Up
*Contact Pair, interaction=IntProp_Mid-Mid
Surf_Up:MidPly_Mid-Bot_U, Surf_Up:MidPly_Mid-Bot_O
**
**
** Interaction: Inter_TopPly-MidPly_Low
*Contact Pair, interaction=IntProp_Mid-Out
Surf_Low:TopPly_Bot-MidPly_Top_U, Surf_Low:TopPly_Bot-MidPly_Top_O
**
**
** Interaction: Inter_TopPly-MidPly_Up
*Contact Pair, interaction=IntProp_Mid-Out
Surf_Up:TopPly_Bot-MidPly_Top_U, Surf_Up:TopPly_Bot-MidPly_Top_O
**
**
** Interaction: Inter_TopPly_1_Low
*Contact Pair, interaction=IntProp_Out-Out
Surf_Low:TopPly_Top-Mid_U, Surf_Low:TopPly_Top-Mid_O
**
**
** Interaction: Inter_TopPly_1_Up
*Contact Pair, interaction=IntProp_Out-Out
Surf_Up:TopPly_Top-Mid_U, Surf_Up:TopPly_Top-Mid_O
**
**
** Interaction: Inter_TopPly_2_Low
*Contact Pair, interaction=IntProp_Out-Out
Surf_Low:TopPly_Mid-Bot_U, Surf_Low:TopPly_Mid-Bot_O
**
**
** Interaction: Inter_TopPly_2_Up
```

```
*Contact Pair, interaction=IntProp_Out-Out
Surf_Up:TopPly_Mid-Bot_U, Surf_Up:TopPly_Mid-Bot_O
**
**------------------------------------------------------------------------------------------
**
**                  STEP: Displacement
**
**------------------------------------------------------------------------------------------
**
*Step, name=Displacement, nlgeom=YES, inc=50000
apply dislacment
*Static
0.1, 5., 5e-05, 5.
**
**------------------------------------------------------------------------------------------
**
**                  BOUNDARY CONDITIONS
**
**------------------------------------------------------------------------------------------
**
** Name: Disp Type: Displacement/Rotation
**
*Boundary
RF, 1, 1, 5.
RF, 6, 6
**
** Name: Fixed Type: Displacement/Rotation
*Boundary
Fixed, 1, 1
Fixed, 2, 2
Fixed, 6, 6
**
**------------------------------------------------------------------------------------------
**
**                  OUTPUT REQUESTS
**
**------------------------------------------------------------------------------------------
**
*Restart, write, frequency=0
**
** FIELD OUTPUT: F-Output-1
**
*Output, field, variable=PRESELECT
**
** HISTORY OUTPUT: H-Output-1
**
*Output, history, variable=PRESELECT
*End Step
**------------------------------------------------------------------------------------------
**------------------------------------------------------------------------------------------
```